
CHICAGO JOURNALS

Spatial and Temporal Variations in Landscape Evolution: Historic and Longer-Term Sediment Flux through Global Catchments

Author(s): J. A. Covault, W. H. Craddock, B. W. Romans, A. Fildani, and M. Gosai

Reviewed work(s):
Source: *The Journal of Geology*, Vol. 121, No. 1 (January 2013), pp. 35-56
Published by: The University of Chicago Press
Stable URL: http://www.jstor.org/stable/10.1086/668680
Accessed: 04/01/2013 11:36

Your use of the JSTOR archive indicates your acceptance of the Terms & Conditions of Use, available at
http://www.jstor.org/page/info/about/policies/terms.jsp

JSTOR is a not-for-profit service that helps scholars, researchers, and students discover, use, and build upon a wide range of content in a trusted digital archive. We use information technology and tools to increase productivity and facilitate new forms of scholarship. For more information about JSTOR, please contact support@jstor.org.


The University of Chicago Press is collaborating with JSTOR to digitize, preserve and extend access to *The Journal of Geology*.

http://www.jstor.org

This content downloaded on Fri, 4 Jan 2013 11:36:15 AM
All use subject to JSTOR Terms and Conditions

Spatial and Temporal Variations in Landscape Evolution: Historic and Longer-Term Sediment Flux through Global Catchments

J. A. Covault,[1,*] *W. H. Craddock,*[2] *B. W. Romans,*[3] *A. Fildani,*[4] *and M. Gosai*[2]

1. Chevron Energy Technology Company, Houston, Texas, U.S.A.; 2. U.S. Geological Survey, Energy Resources, Reston, Virginia, U.S.A.; 3. Department of Geosciences, Virginia Polytechnic Institute and State University, 4044 Derring Hall, Blacksburg, Virginia 24061, U.S.A.; 4. Chevron Energy Technology Company, San Ramon, California, U.S.A.

ABSTRACT

Sediment generation and transport through terrestrial catchments influence soil distribution, geochemical cycling of particulate and dissolved loads, and the character of the stratigraphic record of Earth history. To assess the spatial and temporal variation in landscape evolution, we compare global compilations of stream gauge–derived (n = 1241) and cosmogenic radionuclide (CRN)–derived (predominantly ^{10}Be; n = 1252) denudation of catchments (mm/yr) and sediment load of rivers (Mt/yr). Stream gauges measure suspended sediment loads of rivers during several to tens of years, whereas CRNs provide catchment-integrated denudation rates at 10^2–10^5-yr time scales. Stream gauge–derived and CRN-derived sediment loads in close proximity to one another (<500 km) exhibit broad similarity (n = 453 stream gauge samples; n = 967 CRN samples). Nearly two-thirds of CRN-derived sediment loads exceed historic loads measured at the same locations (n = 103). Excessive longer-term sediment loads likely are a result of longer-term recurrence of large-magnitude sediment-transport events. Nearly 80% of sediment loads measured at approximately the same locations exhibit stream gauge loads that are within an order of magnitude of CRN loads, likely as a result of the buffering capacity of large flood plains. Catchments in which space for deposition exceeds sediment supply have greater buffering capacity. Superior locations in which to evaluate anthropogenic influences on landscape evolution might be buffered catchments, in which temporary storage of sediment in flood plains can provide stream gauge–based sediment loads and denudation rates that are applicable over longer periods than the durations of gauge measurements. The buffering capacity of catchments also has implications for interpreting the stratigraphic record; delayed sediment transfer might complicate the stratigraphic record of external forcings and catchment modification.

Online enhancements: Excel tables, appendixes.

Introduction

A terrestrial catchment is a topographic unit across which sediment is liberated from bedrock, transferred, and/or deposited over variable spatial and temporal scales within a larger sediment-routing system (Allen 1997). A catchment generally includes (1) upland sediment source areas, which can be dominated by denudational processes such as hillslope erosion and river incision; (2) a sediment transfer zone characterized by a river network; and (3) depositional regions along rivers and flood plains, especially in subsiding sedimentary basins (Allen 1997). Sediment routing across landscapes influences soil distribution and global geochemical cycling of particulate and dissolved loads, including a role in the carbon budget and the dispersal of pollutants across continental margins (e.g., Smith et al. 2001; Paull et al. 2002). Perturbations to natural background rates of denudation and sediment flux, perhaps related to historic anthropogenic influences, might (1) alter soil thickness and coverage within a catchment, with implications for the long-term viability of arable regions, and/or (2) accelerate the transfer of sediment, pollutants, and organic carbon to the ocean, with implications for coastline habitats, fisheries, and the global carbon cycle (Syvitski et al. 2005). Sediment flux also de-

Manuscript received September 8, 2011; accepted October 2, 2012.

* Author for correspondence; e-mail: jcek@chevron.com.

[The Journal of Geology, 2013, volume 121, p. 35–56] © 2013 by The University of Chicago. All rights reserved. 0022-1376/2013/12101-0003$15.00. DOI: 10.1086/668680

This content downloaded on Fri, 4 Jan 2013 11:36:15 AM
All use subject to JSTOR Terms and Conditions

fines parameter space for forward stratigraphic models, such as those employed for predictions of petroleum systems (Burgess et al. 2006).

Because of the importance of understanding rates of denudation and sediment flux across Earth's surface, geologists have sought to accurately assess these rates in a breadth of catchment environments (Summerfield and Hulton 1994). One approach has been to compile historic (i.e., generally spanning a single year to decades during the twentieth to twenty-first centuries) suspended-sediment loads from stream gauges and to model loads over longer periods on the basis of present-day geomorphic and climatic conditions (e.g., Milliman and Syvitski 1992; Summerfield and Hulton 1994; Syvitski and Morehead 1999; Syvitski et al. 2003, 2005; Syvitski and Milliman 2007; Milliman and Farnsworth 2011). However, historic-based observations are inherently biased as a result of the influences of anthropogenic catchment modification, including construction of dams and other land-use activities associated with agriculture, construction, and mining (Wilkinson and McElroy 2007). They are also biased according to their relatively short time scale of observation. Sediment gauging–derived loads integrate only the gauging period and are thought to not be applicable to longer time scales (Walling and Webb 1981; Walling 1983; Wittmann et al. 2011). Short gauging periods and low sampling frequencies could result in over- or underestimates of longer-term natural loads, depending on whether significant sediment-transport events were captured during the period of gauge measurements.

Advances in cosmogenic radionuclide (CRN) dating provide catchment-integrated denudation rates and sediment loads at 10^2–10^5-yr time scales (von Blanckenburg 2005). CRNs are produced in situ as secondary cosmic rays interact with rocks within meters of Earth's surface; longer exposure to secondary cosmic rays as a result of slower denudation produces more nuclides. Sediment can be liberated from these rocks, mixed in the catchment through hillslope and fluvial transport processes, and ultimately deposited near the catchment outlet. Accordingly, the CRN abundance measured in sediment deposited near the catchment outlet can be used to divulge the catchment-wide denudation rate, which is inversely proportional to nuclide abundance (Brown et al. 1995; Bierman and Steig 1996; Granger et al. 1996). CRN-derived sediment budgets in large catchments can be complicated as a result of sediment storage in flood plains or other depositional sites (Wittmann and von Blanckenburg 2009). However, recent models of CRN concentration variability across a breadth of active South American flood plains indicate that long-lived CRN concentrations, specifically ^{10}Be and ^{26}Al, remain more or less unchanged during the interval of catchment sediment storage (Wittmann and von Blanckenburg 2009). Thus, a denudation rate of a hinterland can be determined from sediment sampled throughout the entire catchment (Wittmann and von Blanckenburg 2009). CRN-derived sediment budgets might also be complicated because they can encompass glacial-interglacial climate cycles, which influence the spatial distribution and rates of denudation (Schaller and Ehlers 2006; Stock et al. 2009). The degree to which temporal smoothing across these climate cycles biases denudation is poorly understood (Schaller and Ehlers 2006).

Comparison of historic (annual-decadal) to longer-term (predominantly millennial) CRN-derived sediment budgets might provide insights into spatial and temporal variations in landscape evolution that cannot be independently captured by either data set (Summerfield and Hulton 1994). In this contribution, we are motivated by two questions. First, what is the natural range over which denudation rates vary? Such baseline information might be useful for assessing uncertainty of sediment loads measured over various time scales. Second, what general geologic and/or geomorphic characteristics of a catchment, if any, facilitate similarity between denudation and sediment loads measured over decades versus millennia? Furthermore, how might characteristics of a catchment impact the deposits within sediment-routing systems and the signals recorded therein? We will address these questions by comparing compilations of historic, stream gauge–derived denudation rates and sediment loads and longer-term, CRN-derived measurements (predominantly ^{10}Be) of catchment-averaged rates (tables S1 and S2, available in the online edition or from the *Journal of Geology* office; references cited in these tables are listed in appendixes A and B, respectively, which are also available in the online edition or from the *Journal of Geology* office). We investigate entire catchments that drain into the ocean as well as smaller tributaries and subcatchments depending on data availability.

Background

Steady versus Intermittent Sediment Flux. Summerfield and Hulton (1994) demonstrated that for large catchments (in excess of 5×10^5 km^2) sediment load correlates strongly with catchment relief. They inferred that relief is the primary control on sediment flux rates for large regions and that

This content downloaded on Fri, 4 Jan 2013 11:36:15 AM
All use subject to JSTOR Terms and Conditions

sediment flux measured at catchment outlets should be insensitive to the time scale of observation. Of course, elevation and catchment area cannot have a causal link with denudation and sediment load; rather, area and elevation are strongly correlated with other topographic factors that are causally related to sediment flux, namely, gradient and tectonic activity (Milliman and Syvitski 1992; Summerfield and Hulton 1994; Milliman and Farnsworth 2011). The hypothesis of steady sediment flux is contrary to some seminal work on the magnitude and frequency of forcings related to landscape evolution: Wolman and Miller (1960) provided examples of terrestrial catchments in which the majority of sediment is transported during less frequent flows, particularly the 5-yr storm discharge. This begs the question: what is the impact of the centennial or millennial storm on sediment load and denudation measured over different time scales?

Other researchers have demonstrated that episodic phenomena play a key role in landscape evolution in high-standing islands of the southwest Pacific Ocean (Milliman and Meade 1983; Milliman and Syvitski 1992; Lyons et al. 2002; Dadson et al. 2003; Milliman and Farnsworth 2011). These islands include New Zealand, Taiwan, Indonesia, Malaysia, Papua New Guinea, and the Philippines, which collectively make up only ~3% of Earth's landmass. However, the short lengths and steep gradients of the streams and the high variability of rainfall on these islands enable water and sediment to be quickly routed from hinterlands to the ocean (Milliman and Syvitski 1992). Consequently, these high-standing islands might contribute as much as ~35% of the total sediment annually entering the world's oceans (Milliman and Meade 1983; Milliman and Syvitski 1992; Lyons et al. 2002; Milliman and Farnsworth 2011). The sensitivity to external perturbations of catchments across these high-standing islands requires that annual or decadal sediment budgets do not accurately reflect millennial trends, at least in some settings. One reason for the apparent contrasts in the tempo of landscape evolution from one setting to the next may be the contrasting spatial scales at which these studies occur, and we aim to explore this issue with our global compilations of historic and longer-term sediment loads.

Sediment Buffering. One process that may mask the geomorphic processes that govern the tempo of denudation in high-relief hinterlands is the storage of sediment in intercatchment sinks, herein referred to as catchment buffering (e.g., Métivier and Gaudemer 1999; Castelltort and Van Den Driessche 2003; Wittmann et al. 2011). Buffering capacity refers to the degree to which a catchment postpones sediment transfer from hinterland source areas to outlet points in response to an external perturbation (Métivier and Gaudemer 1999; Castelltort and Van Den Driessche 2003; Allen 2008; Wittmann et al. 2011). Postponement of sediment transfer can result from alluviation in flood plains. The larger the proportion of sediment that is sequestered in a catchment during a period of observation, the smaller the sediment flux at the outlet and the smaller the signal of catchment-integrated denudation during that period. In this way, catchment buffering refers to both temporal and spatial lags in sediment transfer. Sediment storage in catchments can persist long enough for lithification, reflected by sedimentary rocks of alluvial origin preserved in the stratigraphic record. Sediment can also be temporarily stored in catchments. Temporary storage can range from 1×10^6–3×10^6 yr in extensive catchments that drain large continental areas (e.g., the Indus River; Clift and Gaedicke 2002) to as brief as decades, centuries, or millennia in smaller catchments with short, steep streams and high variability of rainfall (e.g., high-standing islands of the southwest Pacific Ocean; Milliman and Syvitski 1992; spatially restricted, tectonically active catchments of Southern California; Covault et al. 2010, 2011). Longer-duration sediment storage in larger catchments generally corresponds with greater buffering capacity, and we aim to define the characteristics that favor development of intermediate sediment sinks (e.g., space for deposition in flood plains).

Data and Methods

We compiled historic (annual-decadal) suspended sediment loads (Mt/yr) through catchment outlets predominantly from the global river stream gauge compilation of Milliman and Farnsworth (2011; 774 samples; table S1; figs. 1, 2). Milliman and Farnsworth's (2011) compilation includes rivers that discharge directly into the ocean, rather than tributaries and their subcatchments. Their compilation of rivers includes catchment areas >100 km^2. Potential problems with their database include uneven geographic distribution of rivers, uneven data quality, analytical and reporting errors, inadequate gauging duration to provide a reasonable estimate of average historic suspended-sediment discharge, fewer up-to-date measurements as a result of diminished gauging in recent years, and relatively few dissolved- and bed-load measurements (Milliman and Farnsworth 2011). Milliman

This content downloaded on Fri, 4 Jan 2013 11:36:15 AM
All use subject to JSTOR Terms and Conditions

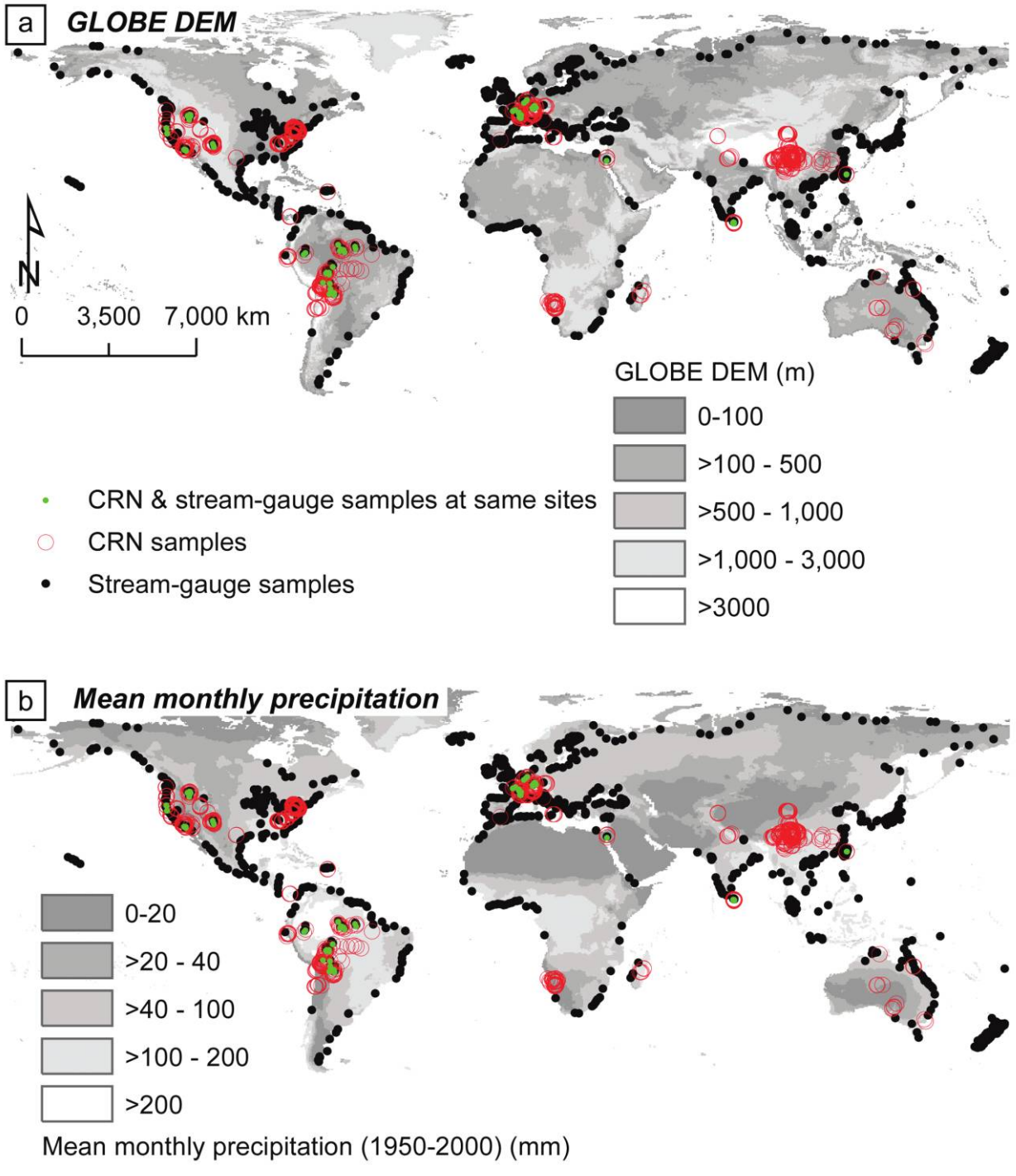

Figure 1. Location maps of stream gauge and cosmogenic radionuclide (CRN) samples. *a*, Samples relative to Global Land One-kilometer Base Elevation Digital Elevation Model (GLOBE DEM; Hastings and Dunbar 1999). *b*, Samples relative to mean monthly precipitation (mm; 1950–2000; Global Historical Climatology Network–Daily 2011). Elevation and precipitation categories follow those of Milliman and Farnsworth (2011).

and Farnsworth (2011) elaborate on these limitations.

To include catchments <100 km^2 in our compilation, we added 219 measurements of average annual suspended sediment load from the U.S. Geological Survey National Water Information System (spanning annual-decadal time scales; USGS Water Data for the Nation 2011; table S1; figs. 1, 2). We

This content downloaded on Fri, 4 Jan 2013 11:36:15 AM
All use subject to JSTOR Terms and Conditions

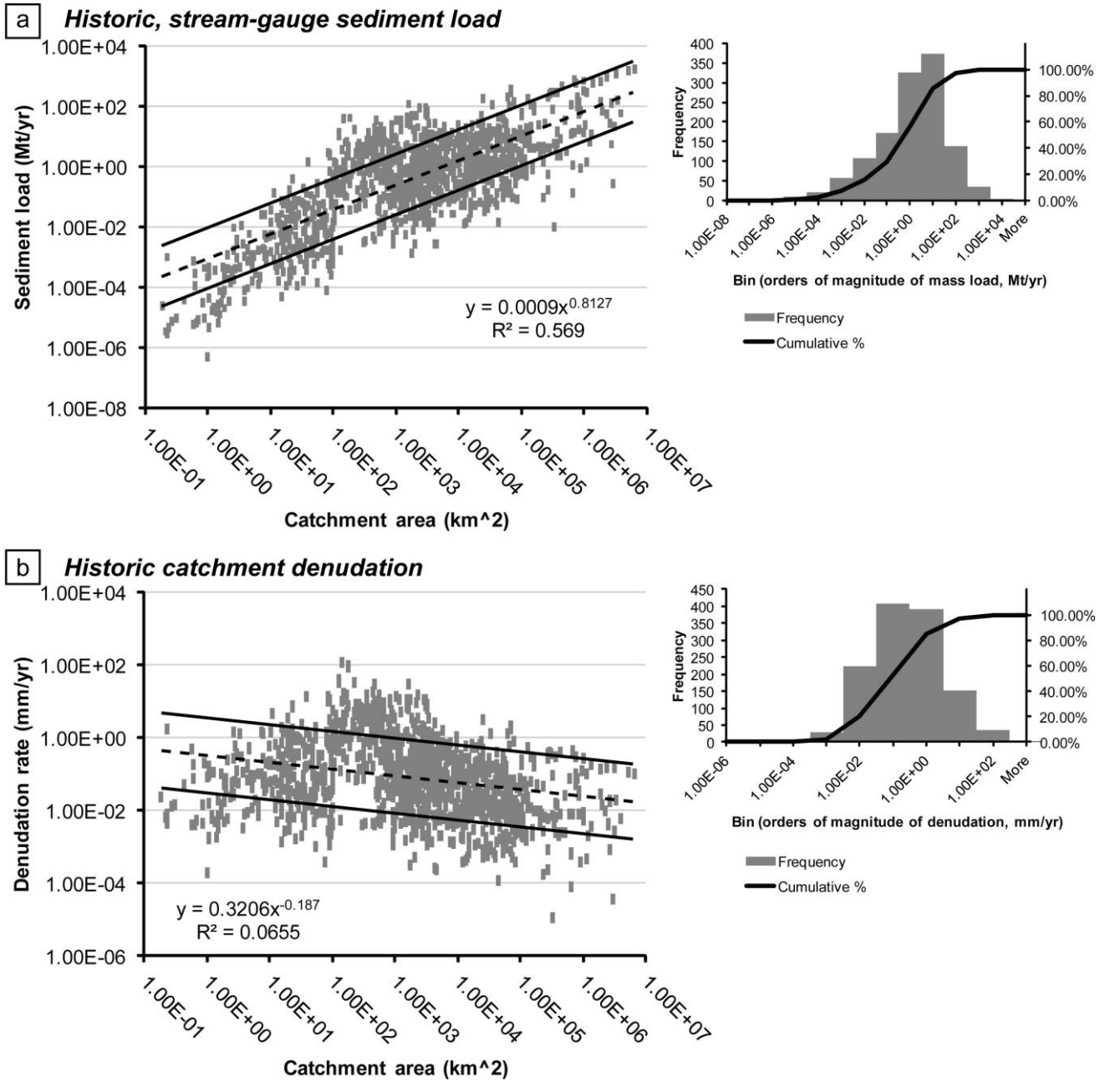

Figure 2. Historic, stream gauge–derived sediment load (*a*) and denudation (*b*) versus catchment area ($n = 1241$; table S1, available in the online edition or from the *Journal of Geology* office). Minimum values are total suspended sediment measurements. Maximum values assume a bed load equal to 50% of the total sediment load. Dashed black lines are best-fitting power functions. Solid black lines define geometric standard deviation envelopes. Histograms of samples are binned according to orders of magnitude of sediment load and denudation. Dissolved loads are not included.

only sampled catchments <100 km^2 from within the 50 states of the United States, the District of Columbia, Puerto Rico, the Virgin Islands, Guam, American Samoa, and the Commonwealth of the Northern Mariana Islands. These samples predominantly include tributaries and subcatchments, rather than larger catchments that discharge directly into the ocean. Moreover, many of these U.S. small-river data are from either lowland (0–500 m elevation) or upland (>500–1000 m elevation) riv-

This content downloaded on Fri, 4 Jan 2013 11:36:15 AM
All use subject to JSTOR Terms and Conditions

ers, which potentially obscures comparison with smaller catchments, including both lowland and upland components, for example, in Taiwan (Milliman and Farnsworth 2011). Many of the problems identified above and elaborated by Milliman and Farnsworth (2011) apply to our sampling of the U.S. Geological Survey database. In particular, >100 gauging stations have been closed annually in the United States since the early 1990s, and sediment discharge measurements of U.S. rivers can be as many as 40 yr old (Lanfear and Hirsch 1999; Milliman and Farnsworth 2011). Additional sources of suspended sediment load data (248 measurements) include publications with companion CRN-derived catchment-integrated denudation rates and two publications of Taiwanese and Nepalese suspended-sediment loads (table S1).

Although total mass load comprises suspended, bed, and dissolved loads, historic catchment-integrated denudation can be estimated using only suspended load (Milliman and Syvitski 1992; Milliman 1997; Burbank 2002; Milliman and Farnsworth 2011). Historic bed load is difficult to measure satisfactorily, and global patterns of river bed-load transport are poorly understood (Allen 1997). Because of the difficulty of measuring bed load, it is common to assume that it is <15% of the suspended load (Milliman and Meade 1983; Summerfield and Hulton 1994; Allen 1997; Burbank 2002). Turowski et al. (2010) suggested that the bed-load fraction of steep, mountainous streams might be 30%–50% of the total sediment load (Galy and France-Lanord 2001; Burbank 2002); however, supporting data from a global distribution of rivers are scarce and of varying quality. We report historic sediment loads as ranges, with the recorded suspended load as a minimum value and up to a 50% bed-load fraction of total sediment load as a maximum (cf. Milliman and Meade 1983; Walling and Webb 1987; Summerfield and Hulton 1994; table S1; fig. 2). That is, we doubled suspended loads to place upper bounds on the range of total sediment loads.

The average annual global delivery of dissolved solids is less than the total sediment load: ~20% of the global budget for suspended sediment (Meybeck 1976; Milliman and Farnsworth 2011). Milliman and Farnsworth (2011) provide estimates of average total dissolved solid loads for only 304 rivers (table S1). We do not include the limited and tenuous measurements of dissolved loads in plots of stream gauge–derived historic sediment load and denudation (Ferrier et al. 2005). We likely overpredict the bed-load component of total sediment load, and the total mass load, including suspended, bed, and dissolved loads, is likely accounted for in the ranges we report (table S1; fig. 2).

If total mass load at a point is known, an average denudation rate (mm/yr) for the upstream catchment can be calculated by normalizing the total load relative to catchment area and converting from mass to length assuming an average rock density of 2.7 t/m^3 (Burbank 2002). We calculate ranges of historic denudation on the basis of ranges of sediment loads, including only suspended loads and up to a 50% bed-load fraction of total sediment load (table S1; fig. 2*b*).

Literature review provided 1252 longer-term, commonly millennial-scale (90% of samples) measurements of catchment-integrated denudation from CRN abundances (predominantly ^{10}Be; table S2; fig. 3). These samples include entire catchments that drain into the ocean as well as smaller tributaries and subcatchments, depending on the particular study. Longer-term mass load is the product of CRN-derived denudation rate, catchment area, and an average rock density of 2.7 t/m^3. A fundamental assumption of CRN analyses is steady state isotopic equilibrium (Bierman and Steig 1996; Brown et al. 1998). Such equilibrium is likely never strictly achieved in many catchments, but changes in sediment generation rates over time are assumed to be well buffered by the soil mantle, where grains might reside for millennia before entering a river (Bierman and Steig 1996; Brown et al. 1998). Furthermore, there is assumed to be no long-term deposition nor change in sediment storage within a catchment (Bierman and Nichols 2004). A sample of sediment at a catchment outlet is also assumed to include CRN abundances representative of the entire catchment as a result of mixing by natural fluvial and hillslope transport processes (von Blanckenburg 2005). Cosmogenic radionuclide production within a catchment (left-hand side below) is balanced by transport out (right-hand side below), as follows:

$$P_0 \Lambda A = \frac{dM}{dt} C, \tag{1}$$

where P_0 is the catchment-integrated (or average) production rate (atoms/yr/g), Λ is the cosmic ray absorption mean free path (at which the intensity of cosmic rays is reduced by a factor of $1/e$ by interaction with material; g/m^2), A is catchment area (m^2), dM/dt is mass flux (g/yr), and C is concentration (atoms/g; von Blanckenburg 2005). Equation (1) can be rearranged to provide catchment-integrated mass flux

This content downloaded on Fri, 4 Jan 2013 11:36:15 AM
All use subject to JSTOR Terms and Conditions

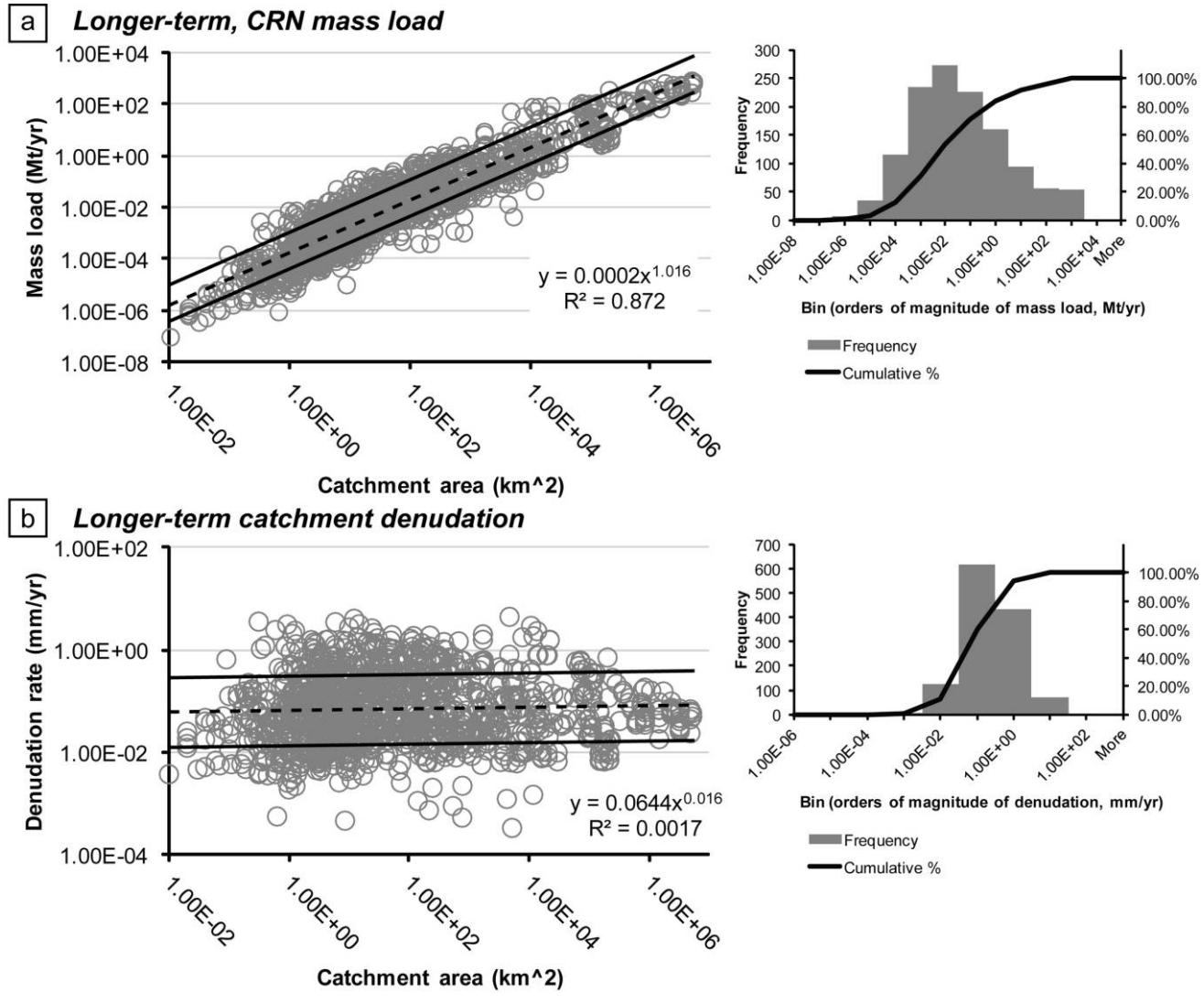

Figure 3. Longer-term, cosmogenic radionuclide (CRN)–derived mass load (*a*) and denudation (*b*) versus catchment area ($n = 1252$; table S2, available in the online edition or from the *Journal of Geology* office). Dashed black lines are best-fitting power functions. Solid black lines define geometric standard deviation envelopes. Histograms of samples are binned according to orders of magnitude of sediment load and denudation.

$$\frac{dM}{dt} = \frac{P_0 \Lambda A}{C} \tag{2}$$

and denudation

$$\varepsilon = \frac{P_0 \Lambda}{C\rho}, \tag{3}$$

where ρ is the density of the catchment substrate material, generally assumed to be 2.7 t/m^3 (Portenga and Bierman 2011).

The majority of data (1097 samples) were from Portenga and Bierman (2011) and references therein. The remaining samples were extracted from the literature, and data were standardized with the CRONUS-Earth online calculator (Balco et al. 2008), following Portenga and Bierman (2011). Unless otherwise specified in the published studies and their supplementary materials, sample thicknesses were assigned a value of 1 cm, geometric shielding factors were assigned a value of 1, and densities were assigned a value of 2.7 g/cm^3 (see Portenga and Bierman 2011). Measurement errors were, on average, <15% of the calculated denudation rates (table S2). Assuming an *e*-folding depth of ~60 cm ($\Lambda/\rho = 160$ g/cm^2/2.7 g/cm^3; Lal 1991; von Blanckenburg 2005), only 129 data points of

This content downloaded on Fri, 4 Jan 2013 11:36:15 AM
All use subject to JSTOR Terms and Conditions

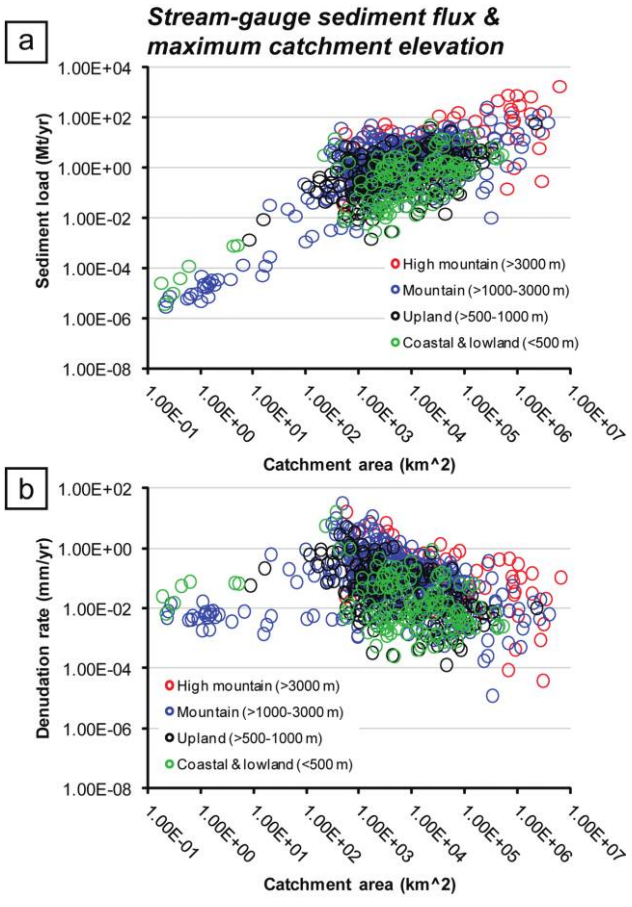

Figure 4. Historic, stream gauge–derived sediment load (*a*) and denudation (*b*) versus catchment area, colored according to the maximum catchment elevation categories of Milliman and Farnsworth (2011; $n = 822$).

our CRN compilation represent less than a millennium of denudation.

One hundred three measurements of denudation and sediment load from stream gauges and CRNs were compiled from approximately the same locations for direct comparisons (fig. 1). Our CRN compilation lacks data from high-standing islands of the southwest Pacific Ocean—New Zealand, Taiwan, Indonesia, Malaysia, Papua New Guinea, and the Philippines, which collectively contribute a significant proportion of sediment to the world's oceans (as much as 35%; Milliman and Meade 1983; Milliman and Syvitski 1992; Lyons et al. 2002; Milliman and Farnsworth 2011). Our compilation includes only eight long-term CRN measurements of sediment load and denudation from a single high-standing island of the southwest Pacific Ocean, Taiwan (Siame et al. 2011; table S2), whereas we compiled 227 historic stream gauge measurements from high-standing islands of the southwest Pacific Ocean (table S1).

Following Milliman and Farnsworth (2011), we attempted to bin sediment-load samples according to maximum catchment elevation: coastal plain (0–100 m), lowland (>100–500 m), upland (>500–1000 m), mountain (>1000–3000 m), and high mountain (>3000 m; figs. 4–7). Eight hundred twenty-two historic stream gauge samples included maximum catchment elevation data, whereas 1115 longer-term CRN samples included elevation data. We also calculated mean monthly precipitation for all catchments (mm; 1950–2000; Global Historical Climatology Network–Daily 2011; figs. 6, 7). The distribution of historic stream gauge loads is skewed to larger values relative to the distribution of longer-term CRN loads; however, the distributions of denudation rates are similar for both stream gauge and CRN data (fig. 8). The distribution of catchment areas is skewed to larger values for stream gauge samples (fig. 8).

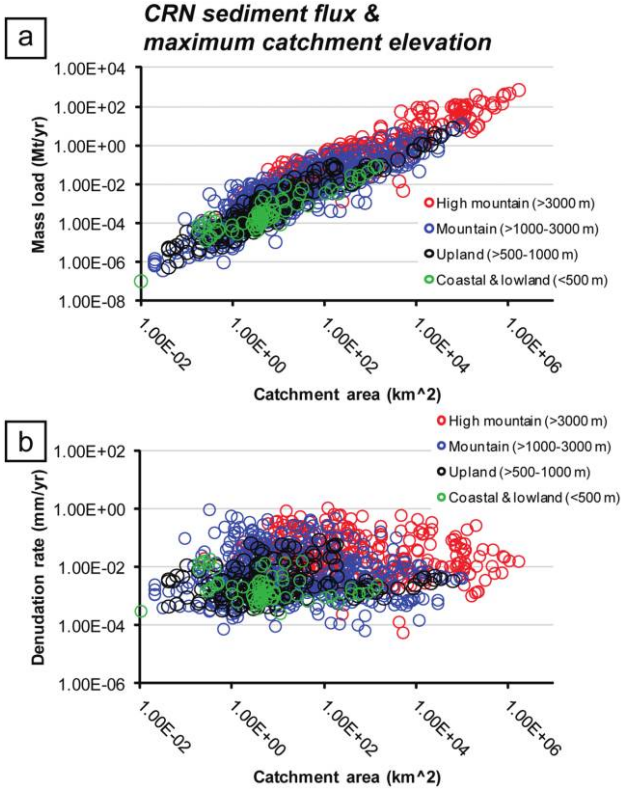

Figure 5. Longer-term, cosmogenic radionuclide (CRN)–derived mass load (*a*) and denudation (*b*) versus catchment area, colored according to the maximum catchment elevation categories of Milliman and Farnsworth (2011; $n = 1115$).

This content downloaded on Fri, 4 Jan 2013 11:36:15 AM
All use subject to JSTOR Terms and Conditions

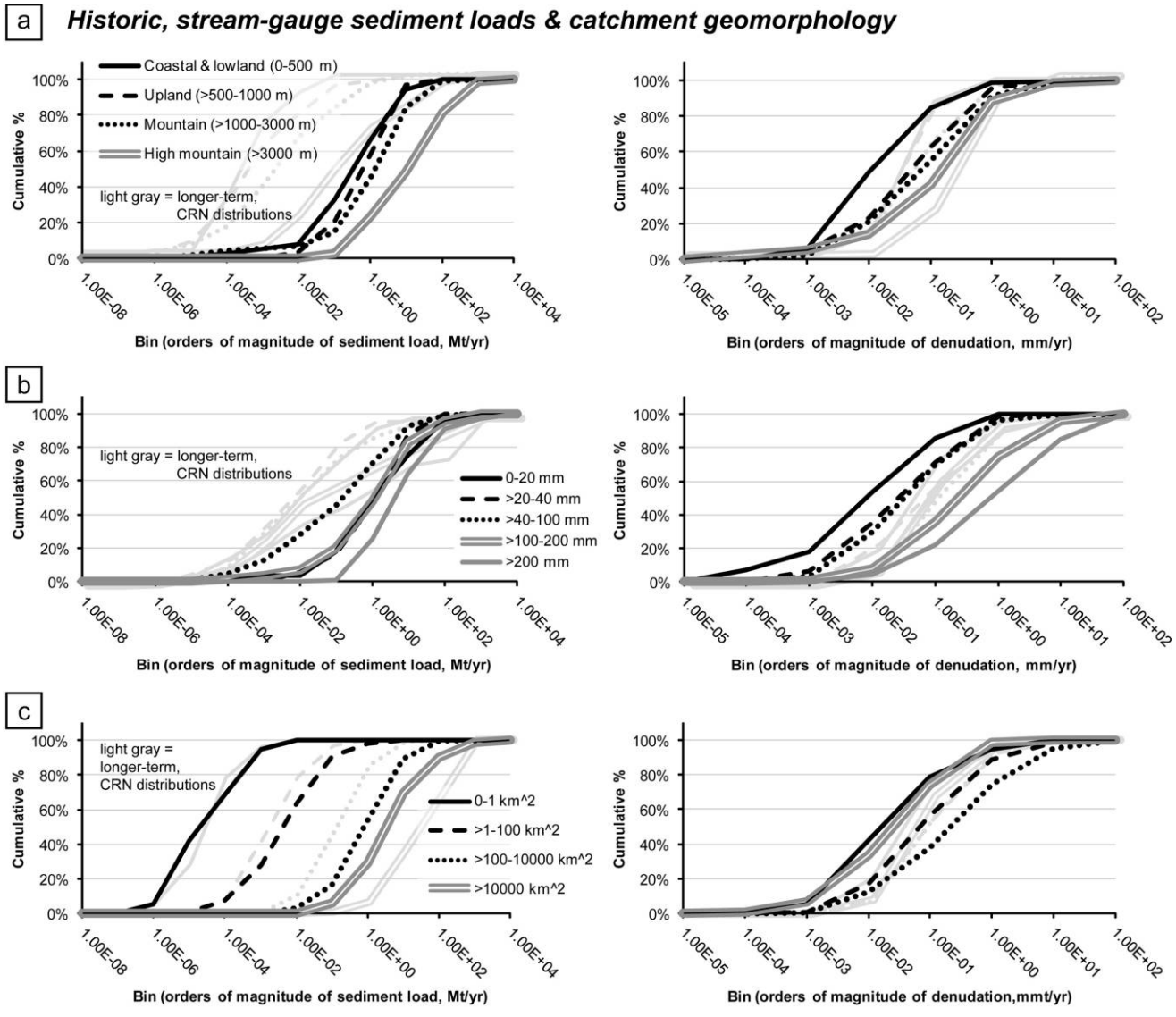

Figure 6. Nonparametric distributions of historic, stream gauge–derived sediment load and denudation by maximum catchment elevation (*a*; $n = 822$), mean monthly precipitation (*b*; $n = 1241$), and catchment area (*c*; $n = 1241$; table S1, available in the online edition or from the *Journal of Geology* office). Elevation (*a*) and precipitation (*b*) categories follow those of Milliman and Farnsworth (2011). Transparent gray curves in the background are similarly categorized distributions of longer-term, cosmogenic radionuclide (CRN)–derived sediment loads and denudation rates for comparison (see fig. 7).

Sediment Loads and Denudation of Catchments

Historic, Stream Gauge–Derived Sediment Flux. Historic, stream gauge–derived sediment loads range from ~1 t/yr to nearly 10 Gt/yr in catchments that range from <1 to nearly 1×10^7 km^2 (table S1; figs. 2*a*, 6*c*, 8). Historic denudation rates range from ~10^{-5} to ~10^2 mm/yr (table S1; figs. 2*b*, 6*c*, 8). Historic sediment loads generally increase with catchment area (figs. 2*a*, 6*c*). Denudation is measured to be most rapid in catchments between ~10^2 and ~10^3 km^2 (figs. 2*b*, 6*c*). These rapid denudation rates are predominantly from high-standing islands of the southwest Pacific Ocean. The standard deviation from best-fitting power functions is approximately plus or minus an order of magnitude for both historic loads and denudation (fig. 2). Figure 4*a* shows that coastal, lowland, and upland catchments (<1000 m elevation) are generally more areally restricted, with smaller sediment loads, relative to more mountainous catchments (see also cumula-

This content downloaded on Fri, 4 Jan 2013 11:36:15 AM
All use subject to JSTOR Terms and Conditions

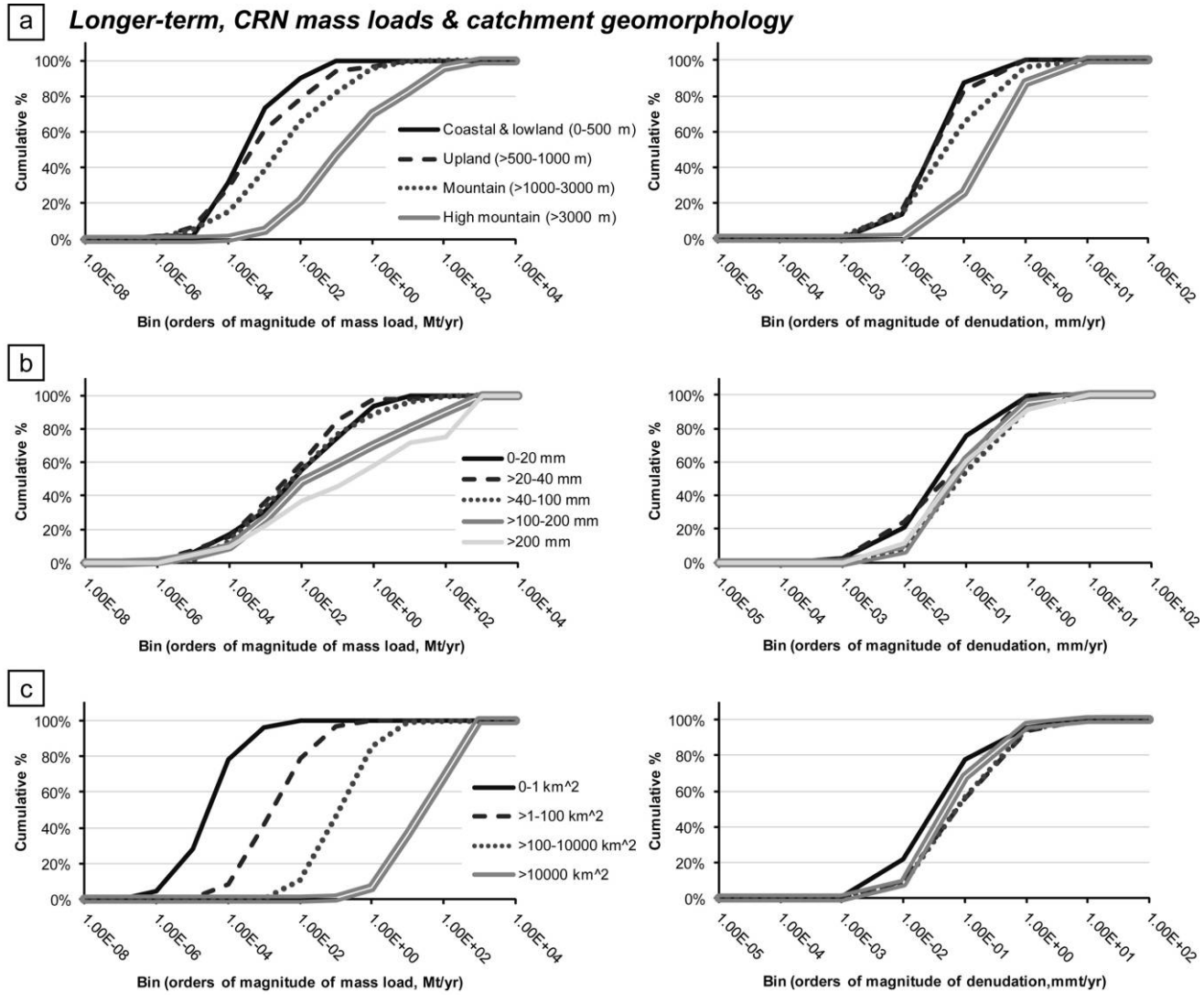

Figure 7. Nonparametric distributions of longer-term, cosmogenic radionuclide (CRN)–derived sediment load and denudation by maximum catchment elevation (*a*; $n = 1115$), mean monthly precipitation (*b*; $n = 1252$), and catchment area (*c*; $n = 1252$; table S2, available in the online edition or from the *Journal of Geology* office). Elevation (*a*) and precipitation (*b*) categories follow those of Milliman and Farnsworth (2011).

tive distributions of fig. 6*a*). Denudation also appears to be slightly more rapid in mountainous catchments, but the relationship is less clear (figs. 4*b*, 6*a*). There does not appear to be a clear relationship between mean monthly precipitation and sediment load; however, more rapid denudation appears to correspond with increasing precipitation according to cumulative distributions of denudation defined by precipitation categories (fig. 6*b*).

Longer-Term, CRN-Derived Sediment Flux. CRN-derived mass loads range from ~1 t/yr to ~1 Gt/yr in catchments that range from ~1×10^{-2} to nearly 1×10^{7} km^2 (table S2; figs. 3*a*, 7*c*, 8). Similar to stream gauge loads, CRN loads increase with catchment area. CRN-derived denudation rates range from ~10^{-2} to ~10 mm/yr (figs. 3*b*, 7*c*, 8). The standard deviation from best-fitting power functions is approximately plus or minus a factor of five for both CRN loads and denudation (fig. 3). Similar to stream gauge data, figure 5*a* shows that coastal, lowland, and upland catchments are more areally restricted, with smaller sediment loads, relative to more mountainous catchments (see also cumulative distributions of fig. 7*a*). CRN-derived denudation also appears to be more rapid in mountainous catchments (fig. 5*b*). There does not appear to

This content downloaded on Fri, 4 Jan 2013 11:36:15 AM
All use subject to JSTOR Terms and Conditions

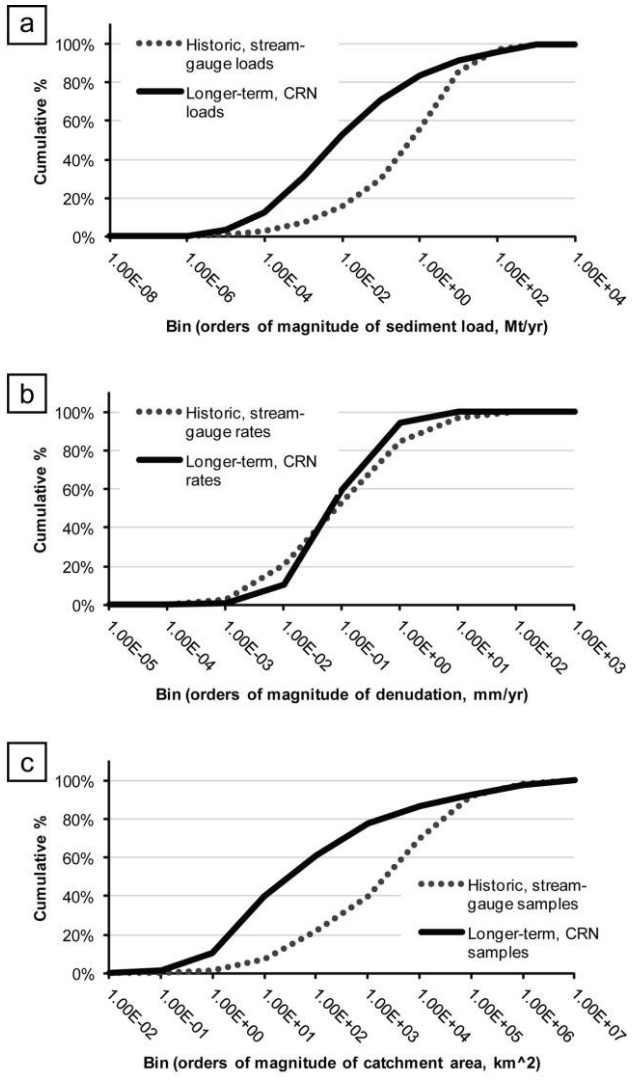

Figure 8. Nonparametric distributions of all stream gauge–derived ($n = 1241$) and cosmogenic radionuclide (CRN)–derived ($n = 1252$) sediment loads (*a*), denudation rates (*b*), and catchment areas (*c*; tables S1, S2, available in the online edition or from the *Journal of Geology* office).

be a clear relationship between mean monthly precipitation and sediment load (fig. 7*b*). The cumulative distributions of denudation defined by elevation, precipitation, and catchment area categories appear to cluster tightly (fig. 7).

Figure 9 shows the best-fitting power functions and standard deviation envelopes for both stream gauge and CRN sediment loads and denudation rates versus catchment area. Historic and longer-term sediment loads appear to overlap and increase with increasing catchment area. However, the range of historic sediment loads is larger than the range of longer-term loads. Historic and longer-term denudation rates are also broadly similar, although historic rates are more variable and exhibit a slight negative relationship with catchment area.

To more meaningfully compare sediment loads and denudation rates measured over vastly different time scales, figures 10 and 11 exhibit plots of measurements from similar regions and approximately the same catchment outlet points (i.e., stream gauge and CRN samples are from the same geographic locations). Figure 10 includes stream gauge and CRN samples within 500 km of one another. As a result, >100 stream gauge samples from high-standing islands of the southwest Pacific Ocean are omitted. Moreover, we chose to omit all Taiwanese samples. There are nearly 30 times more stream gauge samples from rapidly denuding Taiwan,

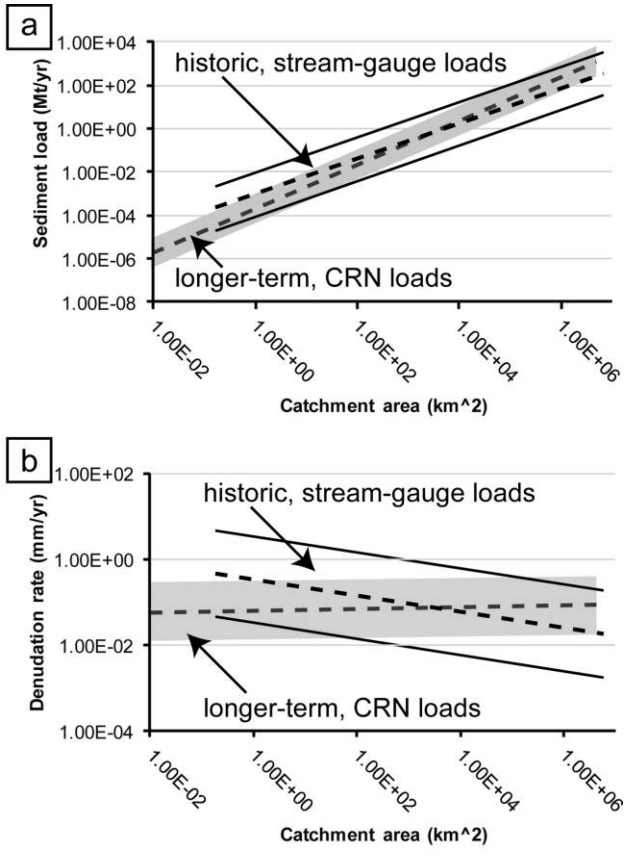

Figure 9. Comparisons of best-fitting power functions and geometric standard deviation envelopes of all stream gauge–derived (based on all 1241 samples) and cosmogenic radionuclide (CRN)–derived (based on all 1252 samples) sediment loads (*a*) and denudation rates (*b*). The standard deviation envelopes of stream gauge data are plotted on top of those of CRN data, which are colored gray. See figures 2 and 3 for scatter plots of all sample data with best-fitting functions and standard deviations.

This content downloaded on Fri, 4 Jan 2013 11:36:15 AM
All use subject to JSTOR Terms and Conditions

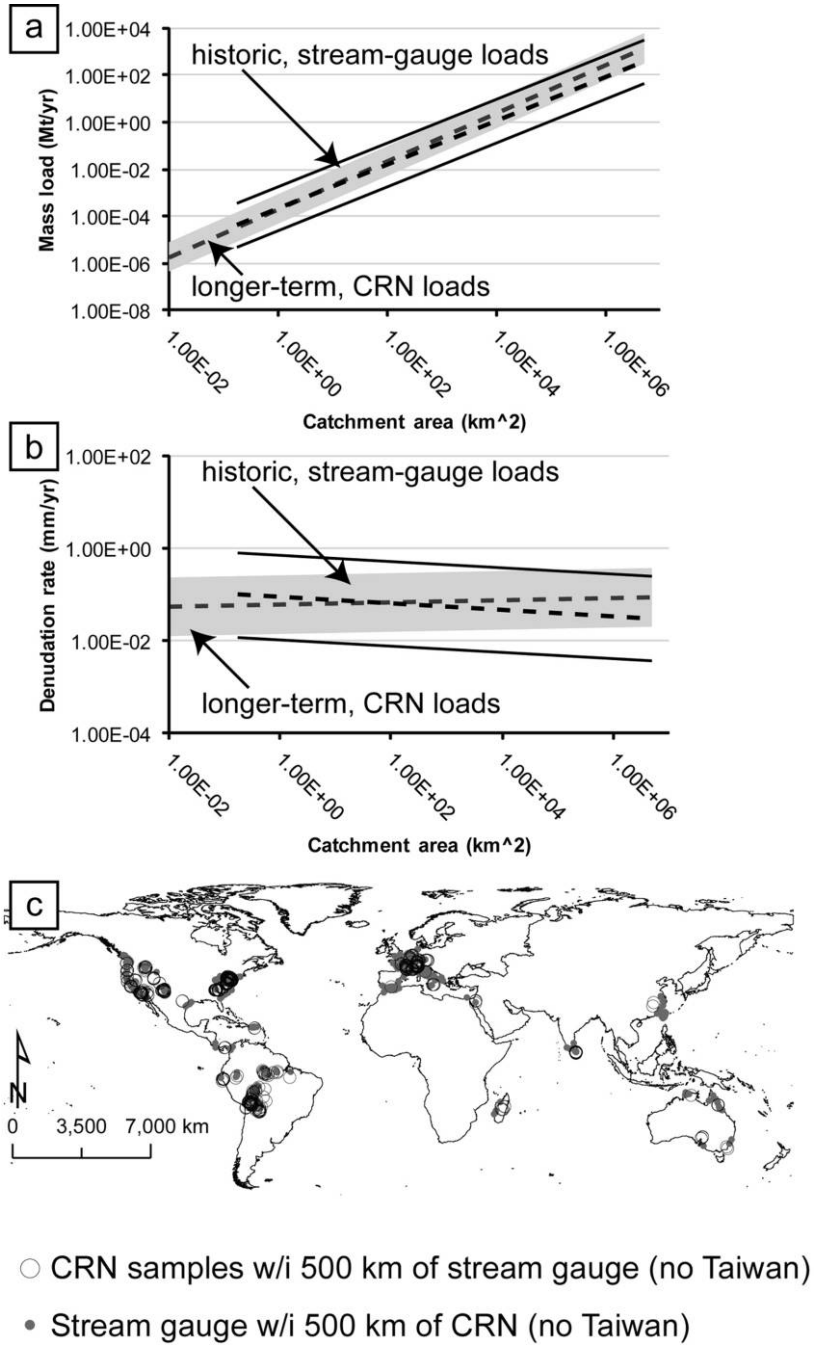

Figure 10. Comparisons of best-fitting power functions and geometric standard deviation envelopes of stream gauge–derived (n = 453) and cosmogenic radionuclide (CRN)–derived (n = 967) sediment loads (*a*) and denudation rates (*b*) within 500 km of each other. Taiwanese data were removed from these compilations. The standard deviation envelopes of stream gauge data are plotted on top of those of CRN data, which are colored gray. Sample locations are shown in *c*.

which obscures comparison to the few CRN samples. Figure 11 shows stream gauge and CRN measurements from the same catchment outlet point. There is broad similarity between sediment loads and denudation rates measured over vastly different time scales: 81 of 103 sites exhibit stream gauge sediment loads that are within an order of magnitude of CRN loads (fig. 9).

This content downloaded on Fri, 4 Jan 2013 11:36:15 AM
All use subject to JSTOR Terms and Conditions

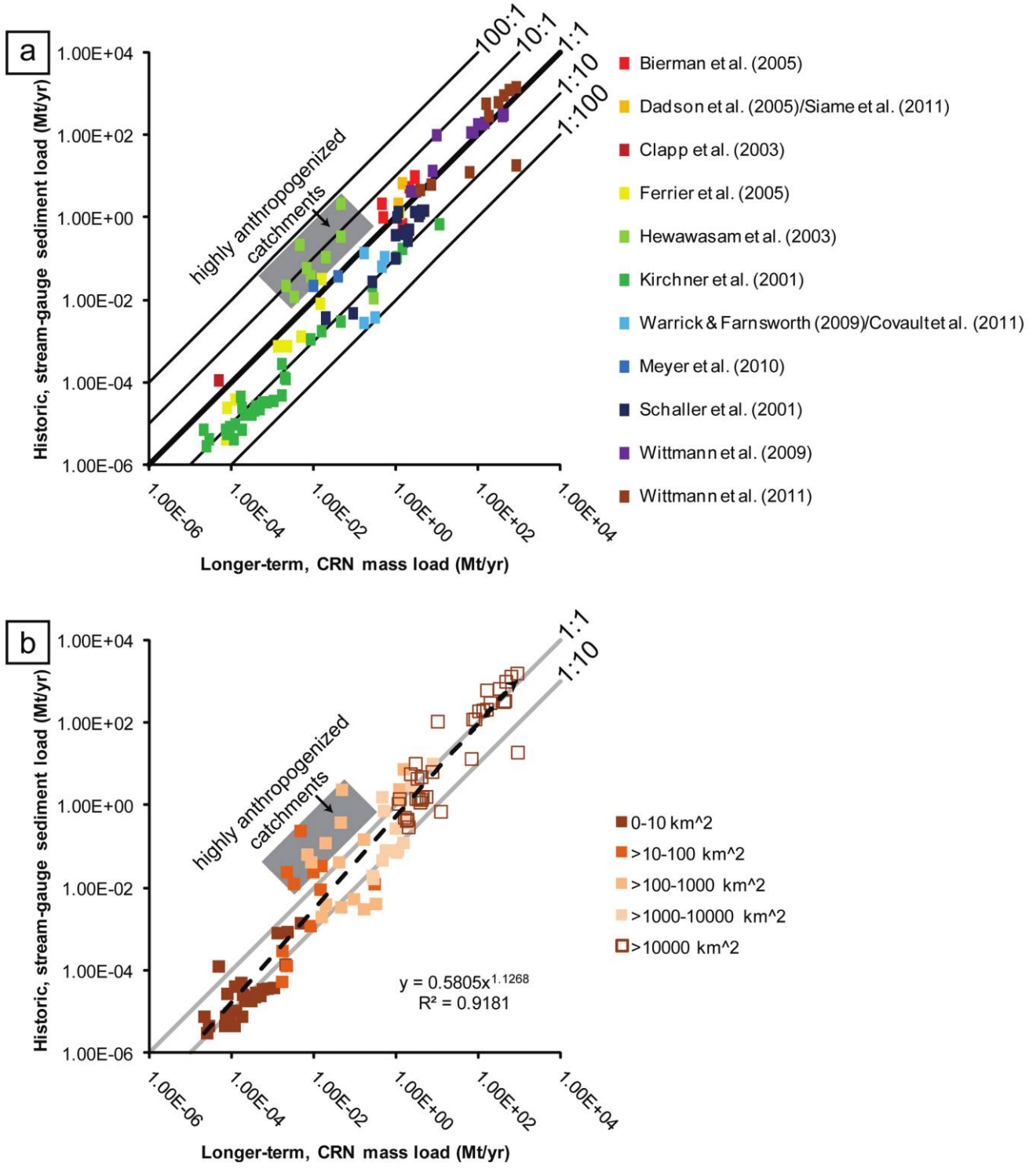

Figure 11. Stream gauge and cosmogenic radionuclide (CRN) samples from approximately the same locations (n = 103). See figure 1 for sample locations. *a*, Sediment loads are colored according to publication source. The vertical height of data points represents the range of historic, stream gauge–derived sediment load. *b*, Sediment loads are colored according to catchment area. The midpoints of the ranges of historic, stream gauge–derived sediment loads are plotted. The dashed black line represents a best-fitting power function.

This content downloaded on Fri, 4 Jan 2013 11:36:15 AM
All use subject to JSTOR Terms and Conditions

Discussion

Sediment Load, Denudation, and Catchment Geomorphology. Historic, stream gauge–derived and longer-term, CRN-derived sediment loads generally increase with catchment area (Milliman and Syvitski 1992; Milliman and Farnsworth 2011; figs. 2–5, 6*c*, 7*c*). This positive relationship likely occurs because larger catchments afford greater surface area for sediment generation and denudation by fluvial-incision, hillslope-erosion, and sediment-transport processes. For example, the Amazon River is the world's largest fluvial system in terms of catchment area and exports 1.2×10^3 Mt/yr of suspended sediment to the Atlantic Ocean during historic time frames (Milliman and Farnsworth 2011; Wittmann et al. 2011). Wittmann et al. (2011) calculated the mass flux through the distal reach of the Amazon River near Obidos to be 0.8×10^3 Mt/yr from CRN abundances, which is remarkably similar to the gauging-derived total suspended-sediment load (figs. 11, 12). In contrast, smaller catchments in tectonically active Southern California exported ~0.3 Mt/yr of total suspended sediment to the Pacific Ocean during historic time frames (Warrick and Farnsworth 2009; figs. 11, 12). Covault et al. (2011) calculated the mass flux through the same Southern California catchments from CRN abundances to be ~1.6 Mt/yr.

There are a number of exceptions to the generalization that larger catchments correspond with larger sediment loads (Milliman and Farnsworth 2011). Our compilation shows that both stream gauge–derived and CRN-derived sediment loads can vary by several orders of magnitude for a given catchment area (figs. 2, 3, 6*c*, 7*c*). Milliman and Farnsworth (2011) showed that the Waiapu River of New Zealand, which has a catchment area of 1.7×10^3 km^2, discharges ~26 times more sediment than the much larger Murray-Darling River (1.1×10^6 km^2) during a historic period of stream gauging. The São Francisco and Brahmaputra Rivers drain similar-sized catchments—6.4×10^5 and 6.7×10^5 km^2, respectively—but have vastly different historic annual sediment fluxes: 6 and 540 Mt/yr, respectively (Milliman and Farnsworth 2011).

The disparity in sediment loads for a given size of catchment is at least partially attributed to differences in maximum elevation of the catchment (Milliman and Syvitski 1992; Bierman and Nichols 2004; Milliman and Farnsworth 2011; figs. 4*a*, 5*a*, 6*a*, 7*a*). In general, mountainous catchments (>1000 m elevation) exhibit larger sediment loads (figs. 4*a*, 5*a*, 6*a*, 7*a*). Of course, elevation and catchment area cannot have a causal link with sediment load; rather, area and elevation are correlated with other topographic factors that are causally related to sediment flux, namely, gradient and tectonic activity (Milliman and Syvitski 1992; Summerfield and Hulton 1994; Bierman and Nichols 2004). The global CRN-derived catchment denudation compilation of Portenga and Bierman (2011) shows that combined environmental parameters, including latitude, precipitation, temperature, and vegetation cover in addition to topographic factors, account for variation in denudation, with average catchment slope being the most significant regressor (table S2).

There does not appear to be a clear relationship between mean monthly precipitation (1950–2000) and either historic or longer-term sediment loads (figs. 6*b*, 7*b*). The impact of mean precipitation on sediment load and denudation is contentious (see the discussion on p. 35–38 in Milliman and Farnsworth 2011; Ahnert 1970). Mean monthly precipitation measured during the twentieth century might not be applicable to longer-term millennial sediment loads or denudation. Over shorter historic time scales, mean monthly precipitation or annual precipitation alone might not be useful in predicting sediment load. Rather, a measure of precipitation seasonality, which considers deviations from mean precipitation (e.g., Walsh and Lawler 1981), combined with vegetation and geomorphic characteristics of a catchment might more meaningfully correlate with sediment load and denudation (Milliman and Farnsworth 2011).

Consistent with previous compilations of global sediment yield (t/km^2/yr) or denudation (e.g., Milliman and Syvitski 1992), figure 2*b* shows a negative best-fit relationship with catchment area. Milliman and Syvitski (1992) link the negative relationship between yield or denudation and catchment area to steeper gradients and less space available for deposition and storage of sediment within smaller catchments. However, denudation is shown to be most rapid in catchments between ~10^2 and ~10^3 km^2 (figs. 2*b*, 6*c*). These rapid denudation rates are predominantly from high-standing islands of the southwest Pacific (table S1). Recent studies have revealed inconsistent trends of sediment yield or denudation versus catchment area for a variety of reasons, including spatial and temporal variability in climate, lithology, topography, dominant erosion processes, and human land use (for a review, see de Vente et al. 2007;

This content downloaded on Fri, 4 Jan 2013 11:36:15 AM
All use subject to JSTOR Terms and Conditions

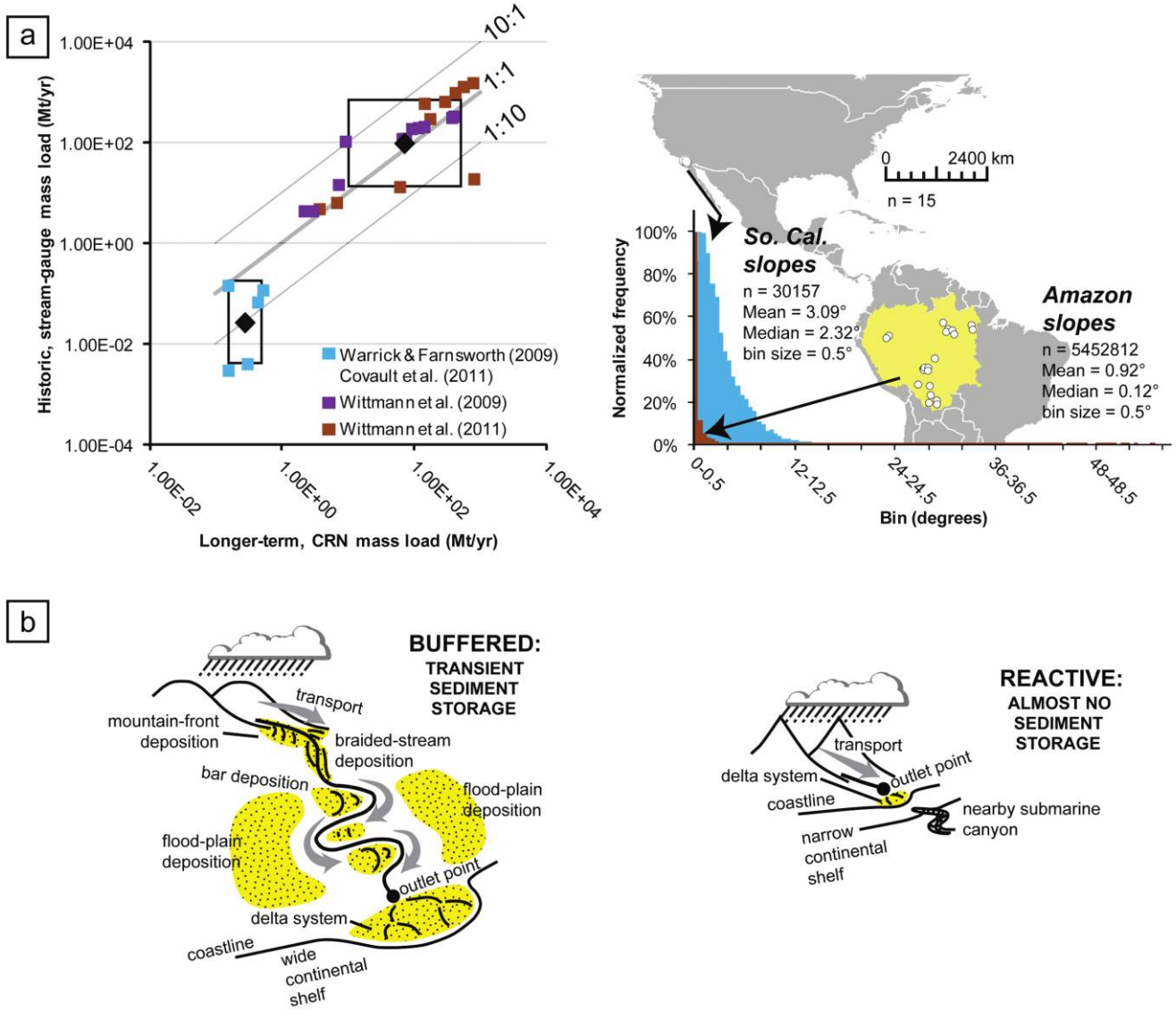

Figure 12. *a*, *left*, Stream gauge–derived and cosmogenic radionuclide (CRN)–derived sediment loads from Southern California, United States, and the Amazon Basin, South America. Black diamonds are geometric means of sediment loads. Black boxes are geometric standard deviations of sediment loads. *a*, *right*, Sample sites and histograms of gradients. *b*, Generalized buffered and reactive catchments.

Saunders and Young 1983; Bierman and Nichols 2004).

Historic versus Longer-Term Sediment Fluxes. Although historic and longer-term data exhibit a broadly similar trend of increasing sediment load with catchment area, historic sediment loads are skewed to larger values relative to longer-term loads (figs. 2, 3, 8*a*). The skew of the distribution of historic sediment loads to larger values is likely because historic data are sampled from larger catchments (fig. 8*c*).

The standard deviation from best-fitting power functions is approximately plus or minus an order of magnitude for both historic loads and denudation, whereas the standard deviation is approximately plus or minus a factor of five for longer-term CRN loads and denudation (figs. 2, 3). The greater variation of the distribution of historic sediment loads likely occurs because (1) historic data span a greater geographic region and, thus, a greater breadth of geomorphology and climate (fig. 1) and (2) CRN data average over longer time periods (von Blanckenburg

This content downloaded on Fri, 4 Jan 2013 11:36:15 AM
All use subject to JSTOR Terms and Conditions

2005; Ivy-Ochs and Schaller 2010). Regarding the second point, the assumption of isotopic as well as geomorphic steady state over long periods (10^2–10^5 yr) is a prerequisite of CRN analyses (von Blanckenburg 2005; Ivy-Ochs and Schaller 2010). However, catchment denudation can vary over shorter periods, and the influx of CRNs into the catchment often is in disequilibrium with the flux out of the catchment. In this common situation, the CRN-derived denudation rate can lag behind variations in catchment denudation, which have changed over time. As a result, changes in denudation over time are smoothed in rates derived from CRN abundances and an average, integrated denudation rate is reported, which might be higher or lower than a shorter-term denudation rate (Ivy-Ochs and Schaller 2010). In particular, cosmogenic budgets of sediment flux that span glacial-interglacial cycles (i.e., 41–100 k.yr.) might overestimate background rates (Schaller and Ehlers 2006). Sediment accumulation rates along the Chilean continental margin suggest that catchment-wide denudation might be ~3 times more rapid during glacial times than during interglacial times (Hebbeln et al. 2007). However, empirical evidence describing the amplitude of fluctuations of denudation and sediment flux across various tectonic and climatic settings remains relatively limited. The point is that longer-term CRN sediment budgets are likely susceptible to similar pitfalls as shorter-term historic budgets, and the steady state assumption over millennia might not always be valid.

Stream gauge and CRN samples within 500 km of one another exhibit similar distributions of sediment load and denudation, even though these data represent landscape evolution spanning vastly different time scales (fig. 10). The standard deviation from best-fitting power functions is approximately plus or minus a factor of eight for both historic loads and denudation, whereas the standard deviation is approximately plus or minus a factor of four for longer-term CRN loads and denudation rates (fig. 10). The similarity in best-fitting functions and variation of stream gauge and CRN sediment loads and denudation is likely a result of geographic proximity, with broadly similar geomorphic (e.g., catchment area and elevation) and climatic conditions (e.g., latitude, precipitation, and seasonality; fig. 10). However, climatic conditions, such as long-term precipitation patterns and seasonality, can considerably vary from one decade, century, or millennium to another.

Sediment Loads at the Same Locations. Figure 11 shows that sediment loads spanning vastly different time scales can vary by greater than an order of magnitude at approximately the same location. Nearly two-thirds of CRN-derived sediment loads exceed historic loads measured at approximately the same locations (fig. 11). Nearly 80% of sediment loads measured at the same locations exhibit stream gauge loads that are within an order of magnitude of CRN loads (fig. 11). However, data from tropical highlands in Sri Lanka (Hewawasam et al. 2003), a hyperarid catchment in southern Israel (Clapp et al. 2000), and a semiarid, arroyo-dominated catchment in New Mexico consistently exhibit larger historic sediment loads (only 17 of 103 sites; Bierman et al. 2005; fig. 11). In Sri Lanka, excessive historic sediment load has been attributed to anthropogenic acceleration of erosion in agricultural regions. Using CRNs to benchmark natural denudation, Hewawasam et al. (2003) calculated that soil is historically lost 10–100 times faster than it is produced in anthropogenized catchments (fig. 11). These measurements from Sri Lanka exhibit the most excessive historic sediment loads relative to longer-term CRN loads, which demonstrate significant human impact on landscape evolution in Sri Lanka and possibly analogous anthropogenized catchments. Imbalances between historic and longer-term sediment loads in arid basins of southern Israel and New Mexico were interpreted to indicate that these catchments are not in steady state (Clapp et al. 2000; Bierman et al. 2005; fig. 11). Rather, alluvium that has been temporarily stored in catchments is historically evacuated (Clapp et al. 2000; Bierman et al. 2005). Although these catchments exhibit relatively large historic sediment loads, they exceed CRN-derived measurements of sediment load only by factors of ~2–4 (fig. 11). In New Mexico, imbalance between sediment loads is interpreted to be a result of land use and human impact (Gellis et al. 2004) as well as historic high-frequency release of sediment through natural arroyo processes (Bierman et al. 2005).

Idaho mountain catchments exhibit longer-term, CRN-derived sediment loads as many as 30 times more rapid than minimum historic fluxes during 10–84 yr of stream gauging (Kirchner et al. 2001; fig. 11). The imbalance between longer- and shorter-term sediment loads is interpreted to result from extremely intermittent sediment delivery, which is dominated by infrequent, large-magnitude sediment-transport events (Kirchner et al. 2001). Heightened longer-term sediment loads are also calculated for spatially restricted, tectonically active catchments of the Peninsular Ranges of Southern California (Warrick and Farnsworth 2009; Covault et al. 2011). There, CRN-derived measure-

This content downloaded on Fri, 4 Jan 2013 11:36:15 AM
All use subject to JSTOR Terms and Conditions

ments of sediment flux can exceed historic measurements by as many as two orders of magnitude (Warrick and Farnsworth 2009; Covault et al. 2011; figs. 11, 12). Southern California catchments are also characterized by intermittent, large-magnitude sediment transfer. The entire annual sediment load of a Southern California river can be discharged in <25 days, which indicates negligible sediment transport over 90% of the annual gauging time (Warrick and Farnsworth 2009). Inman and Jenkins (1999) highlighted the strong correspondence between intermittent El Niño–Southern Oscillation–induced precipitation and heightened sediment flux during a historic period of stream gauging (regarding sediment fluxes during millennia of El Niño–Southern Oscillation cyclicity, see also Romans et al. 2009; Covault et al. 2010). Moreover, Southern California catchments are extensively anthropogenized (Inman 2008; Warrick and Farnsworth 2009). Damming of Southern California rivers is interpreted to have universally reduced sediment discharge by ~45% (Inman 2008; Warrick and Farnsworth 2009). In these extremely sensitive catchments, historic stream gauging evidently is not able to capture the signal of infrequent, large-magnitude sediment-transport events that recur over centennial to millennial time scales (figs. 11, 12). As a result, historic measurements of sediment flux are deficient relative to longer-term records (Inman and Jenkins 1999; Kirchner et al. 2001; figs. 11, 12).

Twenty-eight sites exhibit broad similarity of rates—that is, historic sediment loads are within a factor of two of longer-term loads (figs. 11, 12). These sites are predominantly from larger catchments and subcatchments of the Amazon Basin of South America (Wittmann et al. 2011). In the Amazon Basin, historic and longer-term sediment loads exhibit broad similarity attributed to limited long-term sediment storage in route to catchment outlets and the buffering capacity of the large flood plain (Wittmann et al. 2011). As introduced above, buffering capacity refers to the degree to which a catchment postpones sediment transfer in response to an external perturbation. This postponement can dampen intermittent, large-magnitude sediment-transport events and signals of external forcings (e.g., climatic variability in sediment source areas and anthropogenic soil erosion) at catchment outlet points (Wittmann et al. 2011). Catchment buffering is discussed below.

Measurements of sediment loads at the same locations are expected to significantly vary (Bierman et al. 2005); however, 81 of 103 sites exhibit historic sediment loads that are within an order of magnitude of longer-term loads (fig. 11). As discussed in the context of the ranges of historic and longer-term loads, a single large-magnitude sediment-transport event, such as those prone to occur in highly anthropogenized catchments (e.g., Hewawasam et al. 2003), can overwhelm the average historic record and yield excessive measurements of historic sediment load and denudation (Bierman and Nichols 2004). This appears to be less common; only 17 sites from anthropogenized catchments consistently exhibit excessive historic sediment loads (fig. 11). Alternatively, if the recurrence of large-magnitude sediment-transport events exceeds the period of stream gauging, CRN-derived measurements of sediment flux and denudation are expected to appear excessive (e.g., Kirchner et al. 2001; Schaller et al. 2001; Bierman and Nichols 2004; Nichols et al. 2005). This is the most common situation evident in figure 11, with longer-term, CRN-derived sediment loads exceeding maximum historic fluxes at nearly two-thirds of sites.

Figure 11*b* shows historic and longer-term sediment loads colored according to catchment area. As shown in figures 2 and 3, sediment loads are greater in larger catchments. A best-fitting power function is also displayed, which indicates that the ratio of historic to longer-term sediment loads trends from excessive longer-term, CRN-derived loads (1 : 10 ratio) to approximately balanced loads measured over vastly different time scales (1 : 1 ratio; fig. 11*b*). This trend also generally follows the transition from small to larger catchments (fig. 11*b*), which suggests that the buffering capacity of flood plains within large catchments might promote broad similarity in loads measured over different time scales. Historic and longer-term sediment loads measured at the same locations were not colored according to other geomorphic and climatic variables, such as maximum elevation, distributions of gradients, and mean monthly precipitation, because they were not available for all 103 sample sites.

Buffering Capacity of Catchments. The role of intermittent extreme events in driving landscape evolution remains contentious. Whereas some studies show centimeters of denudation in response to a single storm (e.g., smaller, rapidly uplifting Taiwanese catchments; Dadson et al. 2003), others suggest that historic (annual-decadal) sediment loads broadly match longer-term fluxes (e.g., major global catchments; Summerfield and Hulton 1994; Métivier and Gaudemer 1999; Wittmann et al. 2011). We posit that the buffering capacity of catchments strongly determines the balance between historic and longer-term measurements of sediment load.

This content downloaded on Fri, 4 Jan 2013 11:36:15 AM
All use subject to JSTOR Terms and Conditions

The buffering capacity is determined by the contribution of sediment supply, driven by external perturbations, relative to intracatchment accommodation for deposition, especially flood plains (fig. 12). Diminished buffering capacity of catchments would be characterized by dominance of intermittent extreme events, resulting in orders-of-magnitude imbalances between historic and longer-term sediment fluxes, which are rare in our compilation (figs. 11, 12). This is reactive sediment-routing behavior, in which sediment and signals of external perturbations are rapidly transferred from source areas to outlets (Allen 2008; fig. 12*b*). These imbalances are typically weighted to excessive longer-term sediment loads, in which extreme sediment-transport events are likely preferentially recorded. Shorter-term historic records likely miss these extreme events. Small, tectonically active, steep catchments draining the Peninsular Ranges of Southern California exhibit as many as two orders of magnitude larger CRN-derived sediment loads relative to historic, stream gauge-derived loads (fig. 12).

Catchments in which accommodation for deposition exceeds sediment supply have greater buffering capacity, which is reflected in broad similarity of rates measured over vastly different time scales (e.g., Métivier and Gaudemer 1999; Wittmann et al. 2011; fig. 12). Larger catchments can retain sediment for longer periods as a result of more accommodation for sediment storage and consequent resistance to complete source-to-outlet sediment transfer in response to short-term, small-magnitude external perturbations, such as relatively brief and local storms or earthquakes (fig. 12*b*). As a result, signals of external perturbations to a catchment can be destroyed or severely diluted upon reaching its outlet. Sediment that is deposited in flood plains or other intermediate reaches of catchments can be eroded and exported to outlet points. Métivier and Gaudemer (1999) suggested that rivers and flood plains proportionally adjust to climate changes and upstream denudation in buffered catchments in which sediment loads are approximately balanced over different time scales. That is, if upstream denudation is reduced, the river might incise its flood plain to keep the sediment flux at the outlet constant (Métivier and Gaudemer 1999). Conversely, if climate changes force greater upstream denudation, the river will use the increased sediment load to recharge its previously excavated flood plain (Métivier and Gaudemer 1999). In this way, the steady transfer of reworked flood-plain sediment to an outlet can be maintained over a range of time scales (Métivier and Gaudemer 1999; Clapp et al. 2000; Phillips 2003; Phillips and Slattery 2006; Wittmann et al. 2011; fig. 11*a*).

Characteristics of these buffered catchments include prolific alluviated regions separating hinterland from outlet, generally larger size, and predominantly smaller gradients (fig. 12*b*). These geomorphic characteristics are present within the Amazon River catchment, which exhibits similar historic and longer-term sediment loads (Wittmann et al. 2011; fig. 12*a*). There is at least one prominent exception to the relationship of approximately balanced historic, stream gauge–dervied and longer-term, CRN-derived sediment loads; one site includes a nearly two orders of magnitude larger CRN sediment load (fig. 12*a*). This discrepancy highlights a challenge of applying CRN-derived denudation to calculations of the mass load of an entire catchment (Wittmann and von Blankenburg 2009; Wittmann et al. 2011). Under most conditions of flood-plain storage within large catchments, sediment conserves the CRN concentration of the eroding source area, where the CRNs have predominantly accumulated (Wittmann et al. 2011). Thus, denudation rates are applicable only to the source area in which the sediment was generated, not the entire, relatively large catchment (Wittmann and von Blankenburg 2009; Wittmann et al. 2011). For consistency in calculations of mass load from CRN-derived denudation, we calculated mass load as the product of a CRN-derived denudation rate, an entire catchment area, and an average rock density of 2.7 t/m^3. We did not encounter many obvious problematic mass load calculations following this methodology, especially in smaller catchments in which sediment is generated in close proximity to outlet points. However, the aforementioned data point of excessive CRN-derived mass load is a result of integrating a denudation rate across an entire catchment area rather than the more local source area (fig. 12*a*). In any case, the majority of the Amazon River catchment samples and their mean sediment loads indicate approximately balanced loads measured over historic and longer time scales. The anomalous data point expands the standard deviation envelope of the distribution of Amazon River catchment sediment loads.

Buffered catchments might be superior locations in which to evaluate anthropogenic influences on landscape evolution. Sediment buffering can provide relatively meaningful historic, stream gauge–based measurements of sediment load and denudation. Moreover, significant imbalances between rates measured over different time scales, with excessive historic rates, might indicate human impact in a characteristically buffered catchment. That is, such a catchment might be large with evidence of significant alluviation, but historic sediment loads mea-

This content downloaded on Fri, 4 Jan 2013 11:36:15 AM
All use subject to JSTOR Terms and Conditions

sured during a period of significant anthropogenic modification might be large relative to longer-term natural loads.

Implications for the Stratigraphic Record. Understanding the buffering capacity of catchments also has implications for predictions of depositional architectures across sediment-routing systems and the utility of stratigraphic records in deciphering Earth history. A characteristically buffered catchment might contain larger tracts of alluvium relative to a more reactive catchment dominated by intermittent extreme sediment transport. Longer residence of sediment in buffered catchments might promote weathering, producing more texturally mature sediment. This sediment can be sequestered within the catchment or dispersed beyond to another segment of a land-to-ocean routing system, eventually coming to rest in accommodation across a continental margin.

The postponement of sediment transfer in buffered catchments also has implications for the propagation of signals of external forcings from source to sink. Jerolmack and Paola (2010) proposed that sediment transport through large, buffered routing systems can act as a nonlinear filter that destroys short-term, small-magnitude external signals of stratigraphic forcing (e.g., climatic and/or tectonic fluctuations). Stratigraphic records within and beyond the outlets of such catchments might not represent the timing and magnitude of forcings. Rather, signals will reflect longer time periods and smaller magnitudes (Métivier and Gaudemer 1999; Castelltort and Van Den Driessche 2003). This potentially complicates the meaning of stratigraphic records across continental margins seaward of major fluvial systems.

However, research from tectonically active, spatially restricted sediment-routing systems of Southern California has demonstrated that continental margin deposition can reflect millennial changes in terrestrial catchments (Romans et al. 2009; Covault et al. 2010). This is because land and deep-sea components of small Southern California systems can be consistently linked, and there is limited accommodation for sediment sequestration in route to marine depositional sites (Covault et al. 2010). High-latitude marine depositional systems are also sensitive to climatic variability associated with glacial to interglacial transitions, during which catastrophic floods can rapidly transport sediment thousands of kilometers from terrestrial source to deep-sea sink. Examples of high-latitude sediment-routing systems include the Columbia River–to–Astoria deep-sea depositional system and the Laurentian Channel and other high-latitude systems of the eastern Canadian margin (Brunner et al. 1999; Zuffa et al. 2000; Normark and Reid 2003; Piper and Normark 2009). Similar to the smaller Southern California systems, higher-latitude systems can, at least temporarily, rapidly transport sediment from source to sink. That is, the extreme sensitivity to subglacial conditions and resultant sedimentary processes of high-latitude systems temporarily facilitate relatively efficient sediment transport to the deep sea. These sediment-routing systems have been characterized as reactive, in which the land- and seascapes rapidly respond in concert to a perturbation (Allen 2008). As a result, changes in the rates and magnitude of marine deposition might faithfully reflect changes in the terrestrial source area (Covault et al. 2010).

Conclusions

Compilations of historic, stream gauge–derived and longer-term, CRN-derived sediment loads and denudation in a global breadth of catchment outlets provide insights into the spatial and temporal variability of landscape evolution. Trends of increasing sediment load with catchment area are likely a result of greater surface area for liberation of sediment from the land surface and its transfer to outlets. Sediment loads and denudation in similar regions and at approximately the same locations exhibit broad similarity measured over different time scales. However, longer-term, CRN-derived sediment loads exceed historic loads at the majority of sites. Excessive longer-term loads at the same locations likely are a result of longer-term recurrence of large-magnitude sediment-transport events. Nearly 80% of historic sediment loads are within an order of magnitude of longer-term loads at the same locations, likely as a result of the buffering capacity of large flood plains. Buffered catchments might exhibit historic, stream gauge–derived measurements of sediment load and denudation that are applicable over longer time scales. The buffering capacity of catchments also has implications for interpreting the stratigraphic record: delayed sediment transfer might complicate signals of external forcings recorded in stratigraphy. Conversely, rapid sediment transfer through catchments might result in marine deposits that reflect changes in the terrestrial source area.

ACKNOWLEDGMENTS

We thank J. Milliman, B. Bookhagen, A. Cyr, and Editor D. Rowley for constructive reviews.

This content downloaded on Fri, 4 Jan 2013 11:36:15 AM
All use subject to JSTOR Terms and Conditions

REFERENCES CITED

Ahnert, F. 1970. Functional relationships between denudation, relief, and uplift in large mid-latitude drainage basins. Am. J. Sci. 268:243–263.

Allen, P. A. 1997. Earth surface processes. Oxford, Blackwell Science, 404 p.

———. 2008. Time scales of tectonic landscapes and their sediment routing systems. Geol. Soc. Spec. Publ. 296: 7–28.

Balco, G.; Stone, J. O.; Lifton, N. A.; and Dunai, T. J. 2008. A complete and easily accessible means of calculating surface exposure ages or erosion rates from ^{10}Be and ^{26}Al measurements. Quat. Geochronol. 3: 174–195.

Bierman, P., and Steig, E. 1996. Estimating rates of denudation using cosmogenic isotope abundances in sediment. Earth Surf. Process. Landf. 21:125–139.

Bierman, P. R., and Nichols, K. K. 2004. Rock to sediment—slope to sea with ^{10}Be—rates of landscape change. Annu. Rev. Earth Planet. Sci. 32:215–255.

Bierman, P. R.; Reuter, J. M.; Pavich, M.; Gellis, A. C.; Caffee, M. W.; and Larsen, J. 2005. Using cosmogenic nuclides to contrast rates of erosion and sediment yield in a semi-arid, arroyo-dominated landscape, Río Puerco Basin, New Mexico. Earth Surf. Process. Landf. 30:935–953.

Brown, E. T.; Stallard, R. F.; Larsen, M. C.; Bourles, D. L.; Raisbeck, G. M.; and Yiou, F. 1998. Determination of predevelopment denudation rates of an agricultural watershed (Cayaguas River, Puerto Rico) using in-situ-produced ^{10}Be in river-borne quartz. Earth Planet. Sci. Lett. 160:723–728.

Brown, E. T.; Stallard, R. F.; Larsen, M. C.; Raisbeck, G. M.; and Yiou, F. 1995. Denudation rates determined from the accumulation of in situ–produced ^{10}Be in the Luquillo Experimental Forest, Puerto Rico. Earth Planet. Sci. Lett. 129:193–202.

Brunner, C. A.; Normark, W. R.; Zuffa, G. G.; and Serra, F. 1999. Deep-sea sedimentary record from the late Wisconsin cataclysmic floods from the Columbia River. Geology 27:463–466.

Burbank, D. W. 2002. Rates of erosion and their implications for exhumation. Mineral. Mag. 66:25–52.

Burgess, P. M.; Lammers, H.; van Oosterhout, C.; and Granjeon, D. 2006. Multivariate sequence stratigraphy: tackling complexity and uncertainty with stratigraphic forward modeling, multiple scenarios, and conditional frequency maps. AAPG Bull. 90:1883–1901.

Castelltort, S., and Van Den Driessche, J. 2003. How plausible are high-frequency sediment supply-driven cycles in the stratigraphic record? Sediment. Geol. 157: 3–13.

Clapp, E. M.; Bierman, P. R.; Schick, A. P.; Lekach, J.; Enzel, Y.; and Caffee, M. 2000. Sediment yield exceeds sediment production in arid region drainage basins. Geology 28:995–998.

Clift, P., and Gaedicke, C. 2002. Accelerated mass flux to the Arabian Sea during the middle to late Miocene. Geology 30:207–210.

Covault, J. A.; Romans, B. W.; Fildani, A.; McGann, M.; and Graham, S. A. 2010. Rapid climatic signal propagation from source to sink in a southern California sediment-routing system. J. Geol. 118:247–259.

Covault, J. A.; Romans, B. W.; Graham, S. A.; Fildani, A.; and Hilley, G. E. 2011. Terrestrial source to deep-sea sink sediment budgets at high and low sea levels: insights from tectonically active southern California. Geology 39:619–622.

Dadson, S. J.; Hovius, N.; Chen, H.; Dade, W. B.; Hsieh M.-L.; Willett, S. D.; Hu, J.-C.; et al. 2003. Links between erosion, runoff variability and seismicity in the Taiwan orogen. Nature 426:648–651.

de Vente, J.; Poesen, J.; Arabkhedri, M.; and Verstraeten, G. 2007. The sediment delivery problem revisited. Prog. Phys. Geogr. 31:155–178.

Ferrier, K. L.; Kirchner, J. W.; and Finkel, R. C. 2005. Erosion rates over millennial and decadal timescales at Caspar Creek and Redwood Creek, northern California coast ranges. Earth Surf. Process. Landf. 30: 1025–1038.

Galy, A., and France-Lanord, C. 2001. Higher erosion rates in the Himalaya: geochemical constraints on riverine fluxes. Geology 29:23–26.

Gellis, A. C.; Pavich, M. J.; Bierman, P. R.; Clapp, E. M.; Ellevein, A.; and Aby, S. 2004. Modern sediment yield compared to geologic rates of sediment production in a semi-arid basin, New Mexico: assessing the human impact. Earth Surf. Process. Landf. 29:1359–1372.

Global Historical Climatology Network–Daily. 2011. http://www.ncdc.noaa.gov/oa/climate/ghcn-daily/index.php.

Granger, D. E.; Kirchner, J. W.; and Finkel, R. 1996. Spatially averaged long-term erosion rates measured from in situ–produced cosmogenic nuclides in alluvial sediments. J. Geol. 104:249–257.

Hastings, D. A., and Dunbar, P. K. 1999. Global Land One-kilometer Base Elevation (GLOBE): digital elevation model, documentation, volume 1.0. Key to geophysical records documentation 34. Boulder, CO, National Oceanic and Atmospheric Administration, National Geophysical Data Center, 138 p.

Hebbeln, D.; Lamy, F.; Mohtadi, M.; and Echtler, H. 2007. Tracing the impact of glacial-interglacial climate variability on erosion of the southern Andes. Geology 35: 131–134.

Hewawasam, T.; von Blanckenburg, F.; Schaller, M.; and Kubik, P. 2003. Increase of human over natural erosion rates in tropical highlands constrained by cosmogenic nuclides. Geology 31:597–600.

Inman, D. L. 2008. Highstand fans in the California borderland: comment. Geology 36:e166, doi:10.1130/G24626C.1.

This content downloaded on Fri, 4 Jan 2013 11:36:15 AM
All use subject to JSTOR Terms and Conditions

Inman, D. L., and Jenkins, S. A. 1999. Climate change and the episodicity of sediment flux of small California rivers. J. Geol. 107:251–270.

Ivy-Ochs, S., and Schaller, M. 2010. Examining processes and rates of landscape change with cosmogenic radionuclides. Radioact. Environ. 16:231–294.

Jerolmack, D. J., and Paola, C. 2010. Shredding of environmental signals by sediment transport. Geophys. Res. Lett. 37:L19401.

Kirchner, J. W.; Finkel, R. C.; Riebe, C. S.; Granger, D. E.; Clayton, J. L.; King, J. G.; and Megahan, W. F. 2001. Mountain erosion over 10 yr, 10 k.y., and 10 m.y. time scales. Geology 29:591–594.

Lal, D. 1991. Cosmic ray labeling of erosion surfaces: in situ nuclide production rates and erosion models. Earth Planet. Sci. Lett. 104:424–439.

Lanfear, K., and Hirsch, R. M. 1999. USGS study reveals a decline in long-term stream gauges. EOS: Trans. Am. Geophys. Union 80:605–607.

Lyons, W. B.; Nezat, C. A.; Carey, A. E.; and Hicks, D. M. 2002. Organic carbon fluxes to the ocean from high-standing islands. Geology 30:443–446.

Métivier, F., and Gaudemer, Y. 1999. Stability of output fluxes of large rivers in South and East Asia during the last 2 million years: implications for floodplain processes. Basin Res. 11:293–304.

Meybeck, M. 1976. Total mineral dissolved transport by world major rivers. Hydrol. Sci. Bull. 21:265–284.

Milliman, J. D. 1997. Fluvial sediment discharge to the sea and the importance of regional tectonics. *In* Ruddiman, W. F., ed. Tectonic uplift and change. New York, Plenum, p. 240–258.

Milliman, J. D., and Farnsworth, K. L. 2011. River discharge to the coastal ocean. Cambridge, Cambridge University Press, 384 p.

Milliman, J. D., and Meade, R. H. 1983. World-wide delivery of river sediment to the ocean. J. Geol. 91:1–21.

Milliman, J. D., and Syvitski, J. P. M. 1992. Geomorphic/tectonic control of sediment discharge to the ocean: the importance of small mountainous rivers. J. Geol. 100:525–544.

Nichols, K.; Bierman, P.; Finkel, R.; and Larsen, J. 2005. Long-term (10 to 20 kyr) sediment generation rates for the Upper Río Chagres Basin based on cosmogenic ^{10}Be. *In* Harmon, R. S., ed. The Río Chagres: a multidisciplinary profile of a tropical watershed. New York, Kluwer, p. 297–313.

Normark, W. R., and Reid, J. A. 2003. Extensive deposits on the Pacific plate from Late Pleistocene North American glacial lake outbursts. J. Geol. 111:617–637.

Paull, C. K.; Greene, H. G.; Ussler, W., III; and Mitts, P. J. 2002. Pesticides as tracers of sediment transport through Monterey Canyon. Geo-Mar. Lett. 22:121–126.

Phillips, J. D. 2003. Alluvial storage and the long-term stability of sediment yields. Basin Res. 15:153–163.

Phillips, J. D., and Slattery, M. C. 2006. Sediment storage, sea level, and sediment delivery to the ocean by coastal plain rivers. Prog. Phys. Geogr. 30:513–530.

Piper, D. J. W., and Normark, W. R. 2009. Processes that initiate turbidity currents and their influence on turbidites: a marine geology perspective. J. Sediment. Res. 79:347–362.

Portenga, E. W., and Bierman, P. R. 2011. Understanding Earth's eroding surface with ^{10}Be. GSA Today 21:4–10.

Romans, B. W.; Normark, W. R.; McGann, M. M.; Covault, J. A.; and Graham, S. A. 2009. Coarse-grained sediment delivery and distribution in the Holocene Santa Monica Basin, California: implications for evaluating source-to-sink flux at millennial time scales. Geol. Soc. Am. Bull. 121:1394–1408.

Saunders, I., and Young, A. 1983. Rates of surface processes on slopes, slope retreat, and denudation. Earth Surf. Process. Landf. 8:473–501.

Schaller, M., and Ehlers, T. A. 2006. Limits to quantifying climate driven changes in denudation rates with cosmogenic radionuclides. Earth Planet. Sci. Lett. 248:138–152.

Schaller, M.; von Blanckenburg, F.; Hovius, N.; and Kubik, P. W. 2001. Large-scale erosion rates from in situ–produced cosmogenic nuclides in European river sediments. Earth Planet. Sci. Lett. 188:441–458.

Siame, L. L.; Angelier, J.; Chen, R.-F.; Godard, V.; Derrieux, F.; Bourlès, D. L.; Braucher, R.; Chang, K.-J.; Chu, H.-T.; and Lee, J.-C. 2011. Erosion rates in an active orogen (NE-Taiwan): a confrontation of cosmogenic measurements with river suspended loads. Quat. Geochronol. 6:246–260.

Smith, S. V.; Renwick, W. H.; Buddemeier, R. W.; and Crossland, C. J. 2001. Budgets of soil erosion and deposition for sediments and sedimentary organic carbon across the conterminous United States. Global Biogeochem. Cycles 15:697–707.

Stock, G. M.; Frankel, K. L.; Ehlers, T. A.; Schaller, M.; Briggs, S. M.; and Finkel, R. C. 2009. Spatial and temporal variations in erosion from multiple geochronometers: Wasatch Mountains, Utah, USA. Lithosphere 1:34–40.

Summerfield, M. A., and Hulton, N. J. 1994. Natural controls of fluvial denudation rates in major world drainage basins. J. Geophys. Res. 99:13,871–13,883.

Syvitski, J. P. M., and Milliman, J. D. 2007. Geology, geography, and humans battle for dominance over the delivery of fluvial sediment to the coastal ocean. J. Geol. 115:1–19.

Syvitski, J. P. M., and Morehead, M. D. 1999. Estimating river-sediment discharge to the ocean: application to the Eel margin, northern California. Mar. Geol. 154:13–28.

Syvitski, J. P. M.; Peckham, S. D.; Hilberman, R.; and Mulder, T. 2003. Predicting the terrestrial flux of sediment to the global ocean: a planetary perspective. Sediment. Geol. 162:5–24.

Syvitski, J. P. M.; Vörösmarty, C. J.; Kettner, A. J.; and Green, P. 2005. Impact of humans on the flux of terrestrial sediment to the global ocean. Science 308:376–380.

Turowski, J. M.; Rickenmann, D.; and Dadson, S. J. 2010.

This content downloaded on Fri, 4 Jan 2013 11:36:15 AM
All use subject to JSTOR Terms and Conditions

The partitioning of the total sediment load of a river into suspended load and bedload: a review of empirical data. Sedimentology 57:1126–1146.

USGS Water Data for the Nation. 2011. http://waterdata.usgs.gov/nwis.

von Blanckenburg, F. 2005. The control mechanisms of erosion and weathering at basin scale from cosmogenic nuclides in river sediment. Earth Planet. Sci. Lett. 237:462–479.

Walling, D. E. 1983. The sediment delivery problem. J. Hydrol. 65:209–237.

Walling, D. E., and Webb, B. W. 1981. The reliability of suspended sediment load data. IAHS Publ. 133:177–194.

———. 1987. Material transport by the world's rivers: evolving perspectives. IAHS Publ. 164:313–329.

Walsh, P. D., and Lawler, D. M. 1981. Rainfall seasonality: description, spatial patterns and changes through time. Weather 36:201–208.

Warrick, J. A., and Farnsworth, K. L. 2009. Sources of sediment to the coastal waters of the Southern California Bight. Geol. Soc. Am. Spec. Pap. 454:39–52.

Wilkinson, B. H., and McElroy, B. J. 2007. The impact of humans on continental erosion and sedimentation. Geol. Soc. Am. Bull. 119:140–156.

Wittmann, H., and von Blanckenburg, F. 2009. Cosmogenic nuclide budgeting of floodplain sediment transfer. Geomorphology 109:246–256.

Wittmann, H.; von Blanckenburg, F.; Maurice, L.; Guyot, J.-L.; Filizola, N.; and Kubik, P. W. 2011. Sediment production and delivery in the Amazon River basin quantified by in situ–produced cosmogenic nuclides and recent river loads. Geol. Soc. Am. Bull. 123:934–950.

Wolman, M. G., and Miller, J. P. 1960. Magnitude and frequency of forces in geomorphic processes. J. Geol. 68:54–74.

Zuffa, G. G.; Normark, W. R.; Serra, F.; and Brunner, C. A. 2000. Turbidite megabeds in an oceanic rift valley recording Jökulhlaups of Late Pleistocene glacial lakes of the western United States. J. Geol. 108:253–274.

This content downloaded on Fri, 4 Jan 2013 11:36:15 AM
All use subject to JSTOR Terms and Conditions